nature biotechnology

ARTICLES

https://doi.org/10.1038/s41587-020-0733-7



# Identification of highly selective covalent inhibitors by phage display

Shiyu Chen[1], Scott Lovell[1], Sumin Lee[1], Matthias Fellner[2], Peter D. Mace[2] and Matthew Bogyo[1,3]✉

**Molecules that covalently bind macromolecular targets have found widespread applications as activity-based probes and as irreversibly binding drugs. However, the general reactivity of the electrophiles needed for covalent bond formation makes control of selectivity difficult. There is currently no rapid, unbiased screening method to identify new classes of covalent inhibitors from highly diverse pools of candidate molecules. Here we describe a phage display method to directly screen for ligands that bind to protein targets through covalent bond formation. This approach makes use of a reactive linker to form cyclic peptides on the phage surface while simultaneously introducing an electrophilic 'warhead' to covalently react with a nucleophile on the target. Using this approach, we identified cyclic peptides that irreversibly inhibited a cysteine protease and a serine hydrolase with nanomolar potency and exceptional specificity. This approach should enable rapid, unbiased screening to identify new classes of highly selective covalent inhibitors for diverse molecular targets.**

The efficacy of many drugs is derived from their ability to bind a single target with high selectivity. While drug discovery efforts have historically focused on reversibly binding molecules, recent success with covalent inhibitors has highlighted their potential as therapeutic agents[1,2]. Covalent drugs have the benefits of simplified pharmacokinetic properties and extended duration of therapeutic action compared to reversibly binding drugs. Covalent modifiers of enzyme active-site residues have also been used as activity-based probes (ABPs) to target and functionally characterize proteases and many other diverse families of enzymes[3,4]. However, the discovery of covalent inhibitors that use reactive electrophiles to covalently bind nucleophilic residues (that is, cysteine, serine and lysine) on proteins has been hindered by the challenge of controlling selectivity. While a small number of ABPs have been successfully designed to target a single enzyme, most react with a subset of related enzymes[3,4]. This is largely due to the conserved active-site regions in many enzyme family members and the use of small-molecule or peptide-like ABPs with limited surface area contacts between the probe and target. This liability has been addressed by linking weakly reactive electrophiles to high-affinity, selective binding elements that limit off-target interactions[1,5]. However, methods to identify sufficiently selective binding elements to pair with a reactive electrophile are often time consuming and unsuccessful. Thus, there is a need for a general approach to directly screen large numbers of ligands for their ability to covalently and selectively bind proteins.

Phage display is well suited for this application as it allows for the rapid generation of billions of peptides of exceptionally high diversity on the surface of phage particles, which can then be iteratively screened against molecular targets[6,7]. However, conventional phage methods are limited in that only simple linear peptides made up of natural amino acid sequences can be screened, and the resulting hits are reversibly binding ligands. The approach described here overcomes these limitations. Inspired by previous work using chemical linkers to produce cyclic and bicyclic peptides on the phage surface[8–11], we developed an approach that can be used to form cyclic peptides and to also introduce a weak electrophile warhead directly on the phage coat protein segment (Fig. 1). Cyclization helps to rigidify the peptide scaffold for increased binding potency and selectivity and to also stabilize the resulting probes. These types of cyclized peptides also tend to adopt secondary structures that more closely mimic a folded protein and, therefore, can bind with a greater surface area of contacts compared to a linear peptide[12], increasing the chances of identifying highly selective ligands.

Here we demonstrate the utility and general applicability of the screening approach using two mechanistically distinct enzyme targets. We chose the tobacco etch virus (TEV) protease because it has well-defined primary sequence selectivity and no reported potent inhibitors[13]. We also chose a recently identified serine hydrolase, fluorophosphonate-binding hydrolases F (FphF), from *Staphylococcus aureus*, which has poorly defined substrate specificity but is likely to be an important virulence factor[14]. Our screening efforts using a cyclization linker containing a cysteine-reactive vinyl sulfone (VS) warhead for TEV (Fig. 1a) and a serine-reactive diphenylphosphonate (DPP) warhead for FphF (Fig. 1b) identified a series of peptide sequences that irreversibly inhibited the targets. Further optimization of these sequences resulted in potent, irreversible inhibitors and a fluorescent probe that showed an exceptionally high degree of specificity over other highly related proteases. Therefore, phage screening has the potential to be a general method for the rapid identification of highly selective and stable covalent binding molecules for diverse molecular targets.

## Results

**Design of the cyclization linker.** Inspired by the use of chemical cyclization linkers to generate phage-displayed monocyclic and bicyclic peptides[8,10], we set out to develop a linker that could be used to drive the formation of constrained cyclic peptides while simultaneously introducing a reactive electrophile directly onto the phage coat protein. The 1,3-dichloroacetone (DCA) linker is effective for cyclizing peptides in solution through reaction with two cysteines and for directly modifying phage-displayed peptides without

[1]Department of Pathology, Stanford University School of Medicine, Stanford, CA, USA. [2]Biochemistry Department, School of Biomedical Sciences, University of Otago, Dunedin, New Zealand. [3]Department of Microbiology and Immunology, Stanford University School of Medicine, Stanford, CA, USA. ✉e-mail: mbogyo@stanford.edu

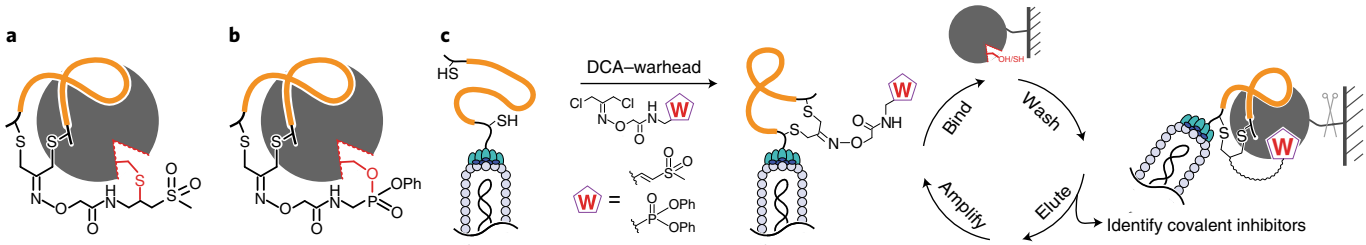


**Fig. 1 | The phage display approach to screen for selective covalent inhibitors. a**,**b**, Schematic of the general strategy to covalently inhibit cysteine and serine hydrolases by peptides (orange) cyclized by linkers containing a reactive VS (**a**) or DPP (**b**) warhead that is presented to the reactive nucleophile (red) of targets. **c**, General workflow of the phage screening method to discover selective covalent inhibitors. The DCA–warhead linkers were used to chemically modify diverse peptides containing two cysteines to generate a cyclic peptide–warhead library on the phage surface. The resulting library can be screened through an iterative process in which phage that covalently bind the target are collected by affinity purification, washed to remove non-covalently bound phage and then eluted by proteolytic digestion. The resulting released phage can then be amplified and subjected to the next round of screening or identified to unveil the sequence of binders.

causing toxicity[11,15]. In addition, the ketone group of DCA allows for convenient derivatization with alkoxy-amines and hydrazines to generate stable oxime and hydrazone linkages to introduce various functional groups[16]. For targeting the cysteine protease TEV, we chose to use a VS electrophile due to its relatively weak reactivity and successful use for covalent inhibition of diverse cysteine protease targets[17]. To avoid any contribution of direct binding to the target protease by the linker itself, we used a glycine VS modified with an aminooxy group for attachment to the DCA linker. We also synthesized a similar analog containing a glycine DPP[18] for use with serine hydrolase targets. We selected the DPP electrophile because it has been used in covalent inhibitors of serine hydrolase targets[18]. Both linkers were synthesized in one step by addition of the aminooxy-linked glycine electrophile to the DCA linker (**11** and **15**, Extended Data Figs. 1 and 2, respectively).

The general screening workflow using the DCA linkers involved treating a library of phage expressing diverse peptides containing two cysteines on their pIII protein and then screening the resulting chemically modified phage for covalent binding to a labeled target (Fig. 1c). To confirm that the DCA–VS and DCA–DPP linkers form the desired cyclic product on phage, we tested their ability to cyclize a dicysteine peptide with a sequence of the form $CX_8C$ (N-ACGSGSGSGCG-C), fused to the N1 and N2 ectodomains of the cysteine-free phage pIII protein[19,20]. After TCEP reduction, the peptide was incubated with either DCA–VS or DCA–DPP, and the cyclization efficiencies were monitored by mass spectrometry (MS)[21]. The results confirmed quantitative and specific cyclization by both linkers in a phage-compatible buffer (Fig. 2a).

**Design of target protease constructs and optimization of washing conditions.** The covalent nature of phage binding to the target provides an opportunity to remove reversibly bound as well as non-specifically bound phage using stringent washing conditions. For releasing covalently bound phage, we engineered an orthogonal protease cut site either on the target protease or on the pIII coat protein of the phage. For the TEV protease, we engineered an expression construct containing an AviTag biotinylation tag attached to its N terminus through a linker recognized by the human rhinovirus 3C protease (EVLFQGP; ref. [22]). To improve the solubility and folding of the TEV protease, we also fused *Escherichia coli* maltose-binding protein through a TEV-cleavable sequence (ENLYFQG) N-terminally to the AviTag[23] (Supplementary Fig. 1). For the FphF protein, we chose to use the native, full-length protein expressed only with an N-terminal HisTag that could be removed after purification through a 3C protease-cleavable site. Because this protein does not contain the AviTag, we performed chemical biotinylation of free lysine residues. This does not allow cleavage of the biotin tag, so we constructed a phage library in which a TEV cleavage site was inserted between the peptide library and the pIII protein to facilitate release of the covalently bound phage (Methods). This approach is optimal for use with targets that do not tolerate a C- or N-terminal tag, are hard to express or can be commercially purchased or purified from native sources (that is, human targets isolated from cells and tissues). To identify optimal wash conditions to remove non-covalently bound phage without causing toxicity, we tested a range of concentrations of guanidine. We found that the infectivity of phage remained high even after treatment with 5 M guanidine chloride (Fig. 2b) and, therefore, used these washing conditions during each stage of the phage screening process.

**Identification of covalently binding cyclic peptide probes that target TEV protease.** For the phage panning experiments with TEV protease, we used a library of phage displaying peptides of eight random amino acids flanked by two cysteines ($CX_8C$; Fig. 3a; ref. [24]). The randomized DNA sequences encoding the peptide library were inserted into the phage DNA between the sequences encoding the pelB signal peptide and the disulfide-free pIII protein in the fdg-3p0ss phage vector[20]. The peptides present on the phage surface were reduced with TCEP and then modified with the DCA–VS linker to generate the cyclic peptide VS (cpVS) phage library. To promote enrichment of stronger and faster binders upon increasing rounds of selection, we allowed phage and biotinylated TEV bound to streptavidin magnetic beads to incubate for 4 h in the first round of selection, 1 h in the second round and 30 min in the third round. Measurement of the overall phage titer levels indicated a slight reduction in phage numbers compared to conventional phage screening, likely due to the stringent 5 M guanidine washes. However, we were able to achieve an approximately 55-fold enrichment in phage numbers through three rounds of panning, suggesting that the selection was successful. To release the selected phage, we incubated the resin with the 3C protease. Phage collected from the third round of selection were used to infect TG1 *E. coli* that were then grown on plates to produce individual colonies for sequencing recovered phage plasmid DNA.

The sequencing results from 19 clones identified consensus peptide sequences that were separated into two groups (Fig. 3b). The first group contained two peptides with a D/ESXQ sequence in the variable seven-residue stretch between the two cysteines (TEV1 and TEV2). The second group contained two peptides with a VXEXLY sequence in an eight-residue stretch between the two cysteines

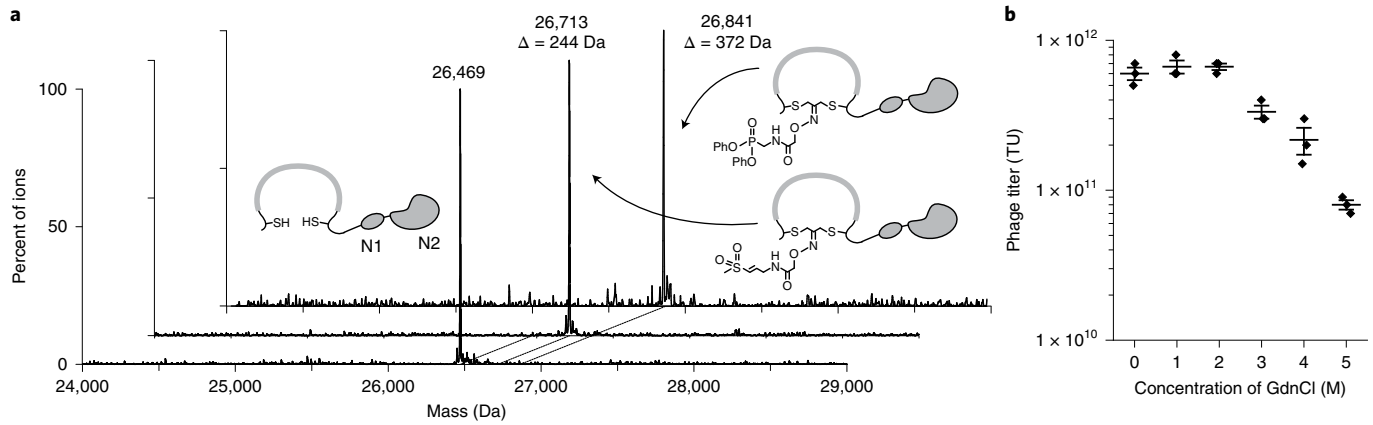


**Fig. 2 | Confirmation of the selectivity and reactivity of the cyclization reactions and establishment of washing conditions for the removal of non-covalently bound phage. a**, A test peptide containing two cysteine residues (N-ACGSGSGSGCG-C) fused to the disulfide-free phage N1 and N2 domains was quantitatively modified to generate the desired cyclic peptide conjugates. The mass shift corresponds to an adduct of a single DCA–VS or DCA–DPP linker. **b**, Plot of phage titers (transducing units, TU) for phage expressing a disulfide-free pIII protein treated with increasing concentrations of guanidine chloride (GdnCl) to determine the highest concentration that could be used in washing steps without causing toxicity to the phage. Assays were performed in triplicate; $n = 3$ biologically independent wells. Data are shown as the mean ± s.d.

(TEV3 and TEV4). This sequence was isolated 17 times from the original 19 colonies. Both sets of sequences contained conserved residues found in the established TEV protease substrate-binding sequence EXLYXQ. To validate the identified sequences, we synthesized all four consensus sequences as linear peptides and then produced the corresponding cyclic peptides by reacting with the DCA–VS linker (Supplementary Fig. 2). To test the inhibitory potency of the cyclized peptides for TEV protease, we used a quenched fluorogenic peptide (Cy5–ENLYFQGK(QSY21)-$NH_2$) as a reporter for protease activity (Fig. 3b and Supplementary Fig. 3). Inhibitors containing the D/ESXQ sequence (TEV1 and TEV2) were an order of magnitude less potent than inhibitors containing the VXEXLY sequence (TEV3 and TEV4). The most potent inhibitor, TEV3, had a half-maximal inhibitory concentration ($IC_{50}$) value of 5 µM, making it an ideal starting point for further optimization to achieve a high-affinity TEV protease inhibitor. To determine which residues of the TEV3 sequence were most important for target binding, we replaced each residue at positions 3–6 and 8–10 with alanine and used glycine to replace the proline at position 7 (Fig. 3c and Supplementary Fig. 2). We found that the conserved glutamic acid at position 6 and leucine at position 8 were essential for binding (TEV5 and TEV7). Mutation of the proline at position 7 and tyrosine at position 9 resulted in a dramatic drop in activity (TEV6 and TEV8). Mutation of any of the other positions only slightly decreased inhibitor potency. We then performed optimization by keeping the essential residues (positions 6–9) while substituting the remaining residues in the peptides with natural amino acids of different sizes, hydrophobicity and electrostatic properties (Supplementary Fig. 4). For positions 3–5, phenylalanine at position 3, methionine at position 4 and glutamine at position 5 showed the most potent inhibition in each group. Modifications at position 10 did not improve potency, so we fixed this position as the original isoleucine. Incorporation of the three preferred amino acids in positions 3–5 into a single peptide sequence resulted in TEV13, which was produced by efficient cyclization with the DCA–VS linker (Supplementary Fig. 5). This inhibitor was the most potent TEV protease inhibitor synthesized, with nanomolar activity against the protease ($IC_{50} = 730$ nM with 1 h of preincubation; Fig. 3d) and a $k_{inact}/K_i$ value of 6,500 ± 130 $M^{-1}$ $s^{-1}$ (Supplementary Fig. 6a).

**Identification of covalent inhibitors with nanomolar potency against FphF.** For screening of the serine hydrolase target FphF, we performed similar steps as described for the TEV protease except that we used a phage library containing a TEV-cleavable linker for release of the covalently bound phage. The library contained a random peptide sequence ($XCX_7C$; Fig. 3e), a short flexible G/S linker (GGSG) and the TEV protease recognition sequence (ENLYFQSG) inserted between the disulfide-free pIII protein and the pelB signal peptide in the fdg3p0ss phage vector[20]. Insertion of the TEV protease cleavage site sequence did not reduce the production yield or infectivity of the phage library.

We performed three rounds of panning against FphF using the same conditions applied to the TEV protease screens. Sequencing of the 19 clones recovered from the third round of selection identified peptides with consensus sequences that were separated into two groups (Fig. 3f). The first group contained four peptides with the sequence QXP at positions 3–5 or 4–6 (FphF1–FphF4). The second group contained three peptides with arginine in position 4 and proline in position 9 (FphF5–FphF7). We synthesized all seven peptides and cyclized them with the DCA–DPP linker (Supplementary Fig. 7). To test the inhibitory potency of these peptides, we used recombinant FphF and a fluorogenic substrate, 4-methylumbelliferyl heptanoate (4-MU heptanoate). The first group of consensus peptides did not show any inhibition of the target at the highest tested concentration of 100 µM. However, the second group of peptides (FphF5–FphF7) showed promising initial activity in the micromolar range, with the most potent peptide, FphF7, inhibiting the enzyme at an $IC_{50}$ value of around 35 µM. This sequence was therefore used as a starting point for further optimization.

To determine the most important residues of FphF7 for target binding, we replaced each of the variable residues with alanine (Fig. 3g) and found that alanine at position 3 (FphF8) greatly improved potency, while replacement of arginine at position 4 and proline at position 9 resulted in a twofold reduction of potency (FphF9 and FphF10). This relatively modest impact of an alanine substitution at the two consensus residues may be due to the fact that the FphF lipid hydrolase is not expected to bind linear peptide substrates, and thus the inhibitor relies on low-affinity interactions between the target and multiple residues of the cyclic peptide. Mutations of other positions did not dramatically change inhibitor potency. We therefore performed optimization of the non-essential positions (positions 5–8) using natural amino acids of different sizes, hydrophobicity and electrostatic properties while keeping position 3 as the optimal alanine, position 4 as arginine and position

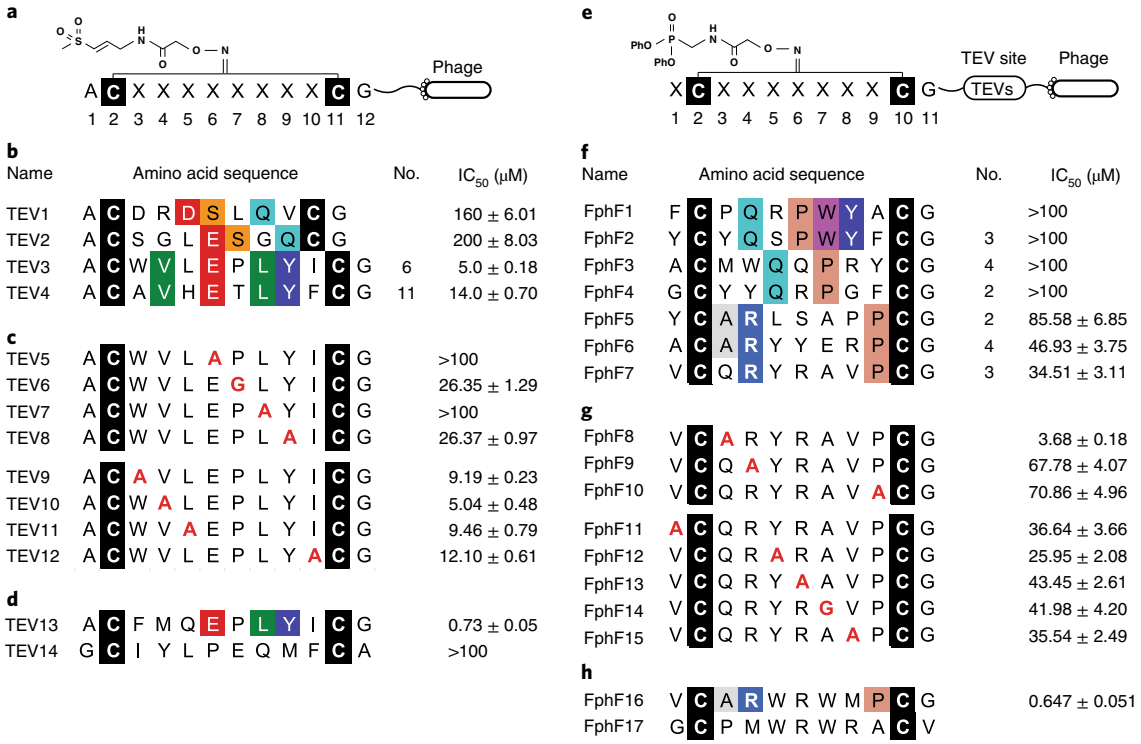


**Fig. 3 | Identification and optimization of covalent cyclic peptide inhibitors of TEV protease and FphF hydrolase. a**,**e**, Schematic of the cyclic peptide phage library generated by cyclizing linear peptides containing two cysteine residues separated by diversity positions ($CX_8C$ or $XCX_7C$) using the cysteine-reactive DCA–VS (**a**) or DCA–DPP (**e**) linker. **b**,**f**, The primary sequences of the cpVS (**b**) and cpDPP (**f**) inhibitors selected after three rounds of panning. The identified sequences are grouped according to sequence similarity. Conserved amino acids are colored using the Shapely coloring rules. For peptides found more than once, the frequency in a pool of the sequenced clones is indicated. Each sequence was chemically synthesized, converted into a cyclic peptide containing the DCA–warhead linker and tested for potency against recombinant TEV protease or FphF hydrolase using a fluorogenic substrate assay. The numbering for the amino acid positions is shown (top). **c**,**g**, Sequences of the peptides used for structure–activity relationship studies to identify key binding residues. The top shows mutations of conserved positions. The bottom shows mutations of positions with non-conserved residues. The $IC_{50}$ values for each of the peptide sequences when converted to the corresponding cpVS or cpDPP inhibitor are shown on the right. **d**,**h**, Sequences and $IC_{50}$ values of the optimized cpVS TEV13 (**d**) and cpDPP FphF16 (**h**) constructed based on the results from the mutational analysis. The mutated residues are shown in red. Data are shown as the average $IC_{50} \pm$ s.d.; $n = 3$ biologically independent wells.

9 as proline. The results indicated that tryptophan at positions 5 and 7, arginine at position 6 and methionine at position 8 showed the most potent inhibition in each group (Supplementary Fig. 8). Incorporation of all four preferred amino acids into a single peptide sequence resulted in an inhibitor, FphF16, with nanomolar activity against FphF ($IC_{50} = 647$ nM with 1 h of preincubation; 95% confidence interval, 785–992 nM; Fig. 3h) and a $k_{inact}/K_i$ value of $27{,}000 \pm 840\ M^{-1}\ s^{-1}$ (Supplementary Fig. 6b).

**Evaluation of cyclic peptide probe and inhibitor specificity.** To demonstrate the selectivity of the optimized inhibitors from the phage screening, we performed inhibition studies using the target proteases and closely related potential off-target proteins. We also synthesized a number of control molecules to further confirm the validity of the panning and optimization processes. For the TEV protease target, we synthesized an isomer of TEV13 in which the order of the amino acid residues between the two cysteines was reversed to rule out inhibition by generic reactivity of the VS electrophile (TEV14; Fig. 4a). We also synthesized a second control containing the optimal TEV13 sequence cyclized with a linker that lacked the reactive VS electrophile (TEV15; Fig. 4a). As a final control, we synthesized a linear heptapeptide VS containing the optimal TEV protease substrate sequence ENLYFQ (TEV16; Fig. 4a). This linear peptide VS probe was synthesized directly on solid support by linking the P1 amino acid of VS through the glutamine side chain to the resin as described previously[25]. Testing of the cyclic peptide controls for inhibition of recombinant TEV protease confirmed that the reversed sequence (TEV14) had no measurable activity even at concentrations as high as 200 μM, and the cyclic peptide lacking the VS warhead (TEV15) showed only weak binding with less than 50% inhibition at concentrations over 200 μM (Fig. 4b). The potency of the optimized inhibitor TEV13 increased with increasing incubation time, consistent with a covalent, irreversible inhibition mechanism (Fig. 4c).

To determine the selectivity of TEV13 compared to the linear peptide TEV16, we tested both against other cysteine proteases. We chose sentrin-specific protease 1 (SENP1) because it has been successfully targeted with a linear peptide VS[26] or the full-length folded SUMO protein[27]. Neither the linear TEV16 nor the cyclic TEV13 was able to inhibit this protease at concentrations as high as 200 μM (Supplementary Fig. 9). We then tested the inhibitors against two cysteine cathepsins (Cat S and Cat L) because both are relatively abundant and active proteases with broad substrate specificity profiles[28] that have been effectively targeted with peptide VSs[29]. We found that the cyclic peptide TEV13 failed to inhibit Cat S or Cat L even when preincubated with the enzymes for 1 h at 37 °C at concentrations over 200 μM (Fig. 4d). In contrast, the linear peptide VS, TEV16, showed highly potent inhibition of Cat L with an $IC_{50}$ value in the low-nanomolar range and substantial inhibition of Cat S when used at high-micromolar concentrations (Fig. 4e).

We then performed similar studies for the optimized FphF inhibitor FphF16 to confirm selectivity. For controls, we used the reverse-sequence cyclic peptide DPP (FphF17; Fig. 4f) and a

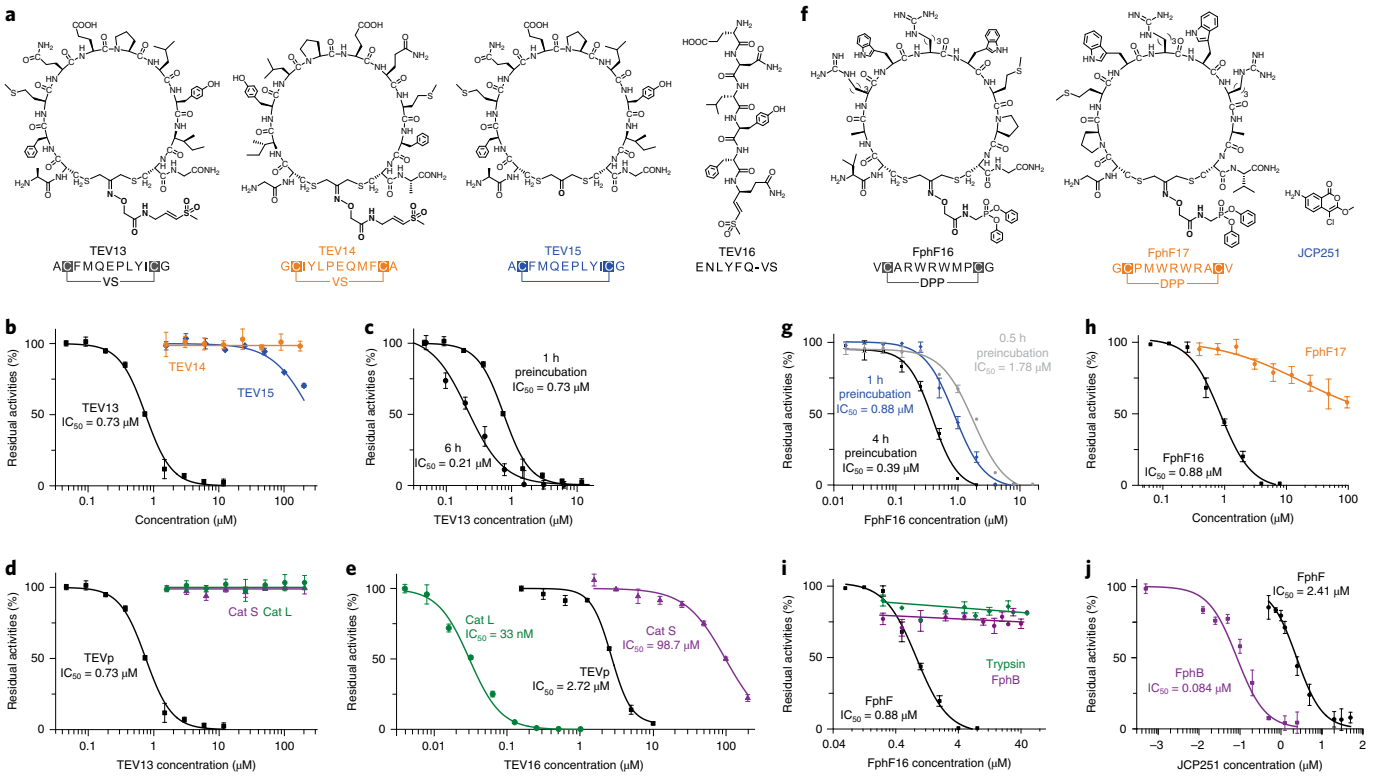


**Fig. 4 | TEV13 and FphF16 are potent and specific covalent inhibitors. a**, Structures of the optimized cpVS inhibitor TEV13 compared to the scrambled isomer (TEV14), the cyclic peptide lacking the VS electrophile in the linker (TEV15) and the linear peptide VS synthesized based on the conserved substrate specificity of TEV protease. **b**, Dose response inhibition studies of the cyclized peptides using recombinant TEV protease. Plots show residual enzyme activity over a range of inhibitor doses as measured by hydrolysis of a fluorogenic substrate. Enzyme was pretreated with inhibitor at the indicated concentrations for 1 h followed by the addition of substrate and measurement of activity. $IC_{50}$ values, when measurable, are indicated. **c**, Time dependence of TEV protease inhibition by TEV13. Recombinant enzyme was preincubated with a range of TEV13 concentrations for 1 h or 6 h as indicated followed by measurement of residual activity using a fluorogenic substrate. **d**,**e**, Comparisons of the activity of TEV13 (**d**) and TEV16 (**e**) for TEV protease and the off-target cysteine proteases Cat S and Cat L. Inhibition studies were performed as in **b**. **f**, Structure of the optimized cpDPP inhibitor FphF16 compared to the sequence-scrambled cpDPP (FphF17) and JCP251, a reported chloroisocoumarin inhibitor of the Fph hydrolases. **g**, Time dependence of FphF hydrolase inhibition by FphF16. FphF16 was preincubated with the recombinant FphF hydrolase for 0.5, 1 and 4 h followed by addition of a fluorogenic substrate, 4-MU heptanoate. The residual enzyme activities represented by the fluorescent signals are plotted. **h**, Dose response of FphF16 and FphF17 to inhibit recombinant FphF hydrolase. $IC_{50}$ values were determined as above. **i**,**j**, Comparisons of the activity of FphF16 (**i**) and FphF17 (**j**) for FphF hydrolase and the off-target FphB hydrolase and trypsin. Inhibition studies were performed as in **g**. $n = 3$ biologically independent wells. Data are shown as the mean ± s.d.

small-molecule chloroisocoumarin inhibitor (JCP251; Fig. 4f) that inhibits a highly related serine hydrolase, FphB, in the same family as FphF[14]. Inhibition of FphF by the optimized inhibitor, Fph16, was time dependent, consistent with a covalent mode of inhibition (Fig. 4g). The reverse-sequence inhibitor, FphF17, showed no measurable inhibitory activity against FphF (Fig. 4h), confirming that the reactive DPP electrophile is not sufficient to promote inhibition of the target enzyme. To further confirm selectivity of the lead molecule, we tested it against several other serine hydrolase targets, including trypsin and FphB. Trypsin is an ideal off-target because it is a highly active and promiscuous protease that can be inhibited by the DPP electrophile[18]. FphB is a stringent control for selectivity because the enzyme has 52% sequence similarity to FphF, and both enzymes have a highly conserved catalytic α/β-hydrolase domain. The FphF16 inhibitor retained absolute specificity for FphF over both trypsin and FphB even when used at concentrations as high as 200 μM (Fig. 4i), while the FphB-selective inhibitor JCP251 showed potent activity for FphB but also low-micromolar potency for FphF (Fig. 4j).

**Generation of a selective ABP from phage-selected inhibitors.** One of the most effective ways to assess the selectivity of a covalently binding molecule is to make a tagged version for labeling complex mixtures containing off-target proteins and other reactive nucleophiles. We therefore conjugated a Cy5 fluorophore to the free N termini of TEV13, TEV14 and TEV16 to generate corresponding fluorescent probes (Fig. 5a). We tested probe labeling of purified TEV protease in buffer and when added to total protein extracts from HEK293 and TG1 cells. The Cy5–TEV13 probe specifically labeled TEV protease alone and when mixed with a complex protein mixture, while the corresponding reverse-sequence probe, TEV14, showed no labeling, consistent with its lack of activity for TEV protease (Fig. 5b). The linear peptide VS probe Cy5–TEV16 effectively labeled TEV protease in buffer and in total protein extracts. However, the intensity of TEV labeling was reduced compared to Cy5–TEV13, and the probe also showed an increased amount of background labeling in the lysates (Fig. 5c). Covalent binding of Cy5–TEV13 and Cy5–TEV16 was dependent on both concentration and incubation time (Supplementary Fig. 10). Furthermore, the TEV protease labeling by Cy5–TEV13 could be blocked by preincubation with the TEV13 inhibitor lacking the Cy5 label (Supplementary Fig. 11). To further assess the selectivity of the probes, we performed labeling of RAW cell extracts with various concentrations of the probes at

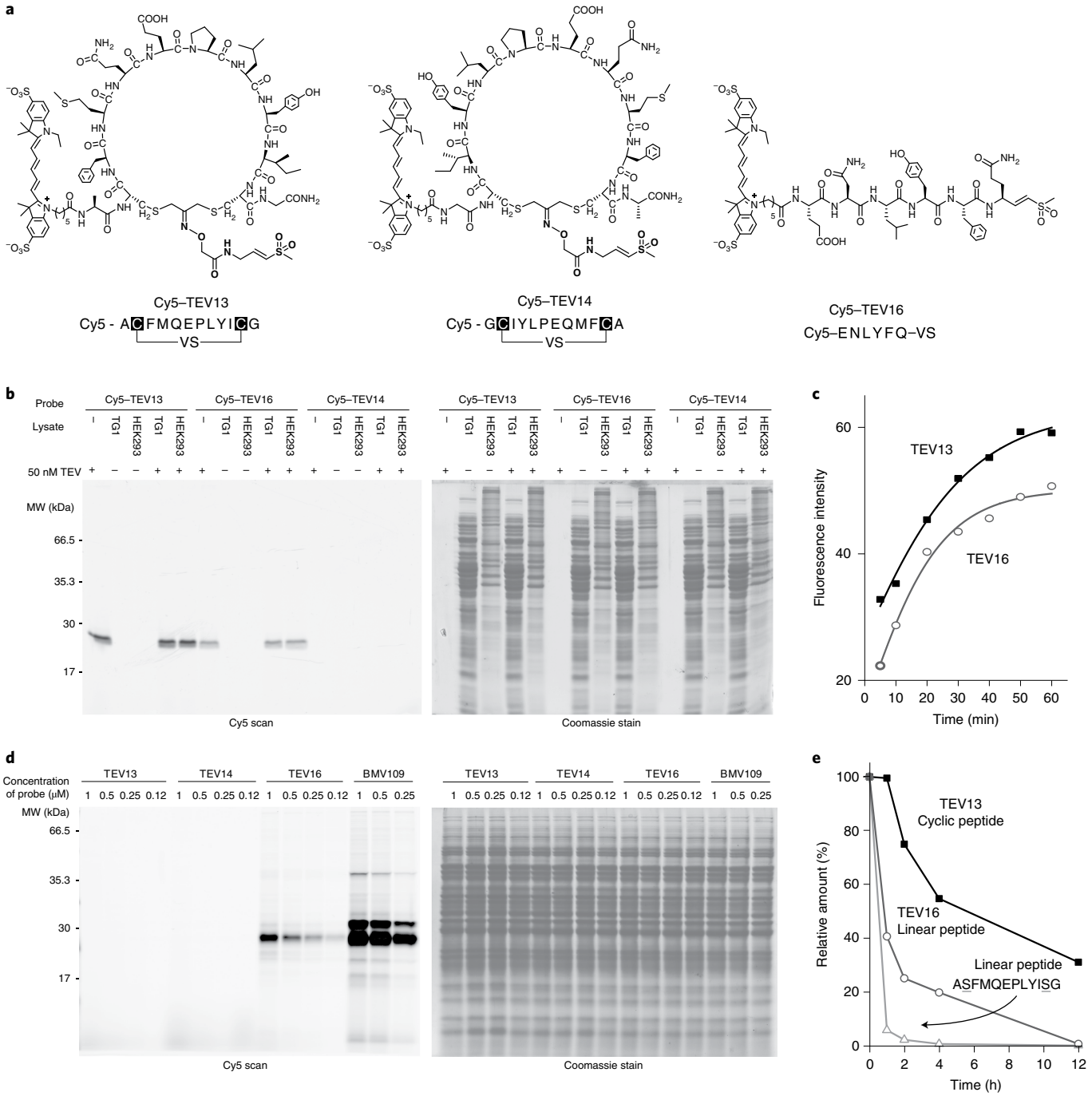


**Fig. 5 | The fluorescent cpABP Cy5–TEV13 specifically labels TEV protease in complex proteomic samples. a**, Chemical structures of the Cy5-fluorophore-labeled ABP versions of the cyclic peptides TEV13 and TEV14 and the linear peptide-VS TEV16. **b**, Samples of enzyme buffer (–) or lysates from TG1 or HEK293 cells (4 μg total protein) were spiked with purified recombinant TEV protease (15 ng) or buffer as indicated followed by addition of the indicated Cy5-labeled probes. Samples were incubated for 1 h at 37 °C and then SDS–PAGE sample buffer was added followed by boiling. Samples were separated on SDS–PAGE gels and scanned for Cy5 fluorescence using a flatbed laser scanner (left) and then stained with Coomassie brilliant blue (right) to visualize total protein loading. **c**, Curves plotting the labeling intensity of recombinant TEV protease (15 ng) in buffer over the range of indicated times. Samples were analyzed by SDS–PAGE followed by scanning of the gel using a flatbed laser scanner to quantify the intensity of labeled protease at each time point. **d**, Images of SDS–PAGE gels containing samples of the indicated total cellular lysates labeled for 1 h with the indicated concentrations of each Cy5-labeled probe. The BMV109 probe is a general ABP for cysteine cathepsins that was included for reference. The gels were processed as in **b**. **e**, Plots of relative levels of each of the indicated cyclic and linear peptides after the indicated incubation time in mouse plasma. Values were obtained by quantification of parent ions by MS.

two pH values. We chose RAW cells because they have high levels of cysteine cathepsin expression[30]. The labeling results confirmed that the Cy5–TEV13 probe retained selectivity at both pH values, with virtually no off-target background labeling even at the highest probe concentrations used. In contrast, the linear peptide Cy5–TEV16 labeled multiple cathepsins even at the lowest probe concentration

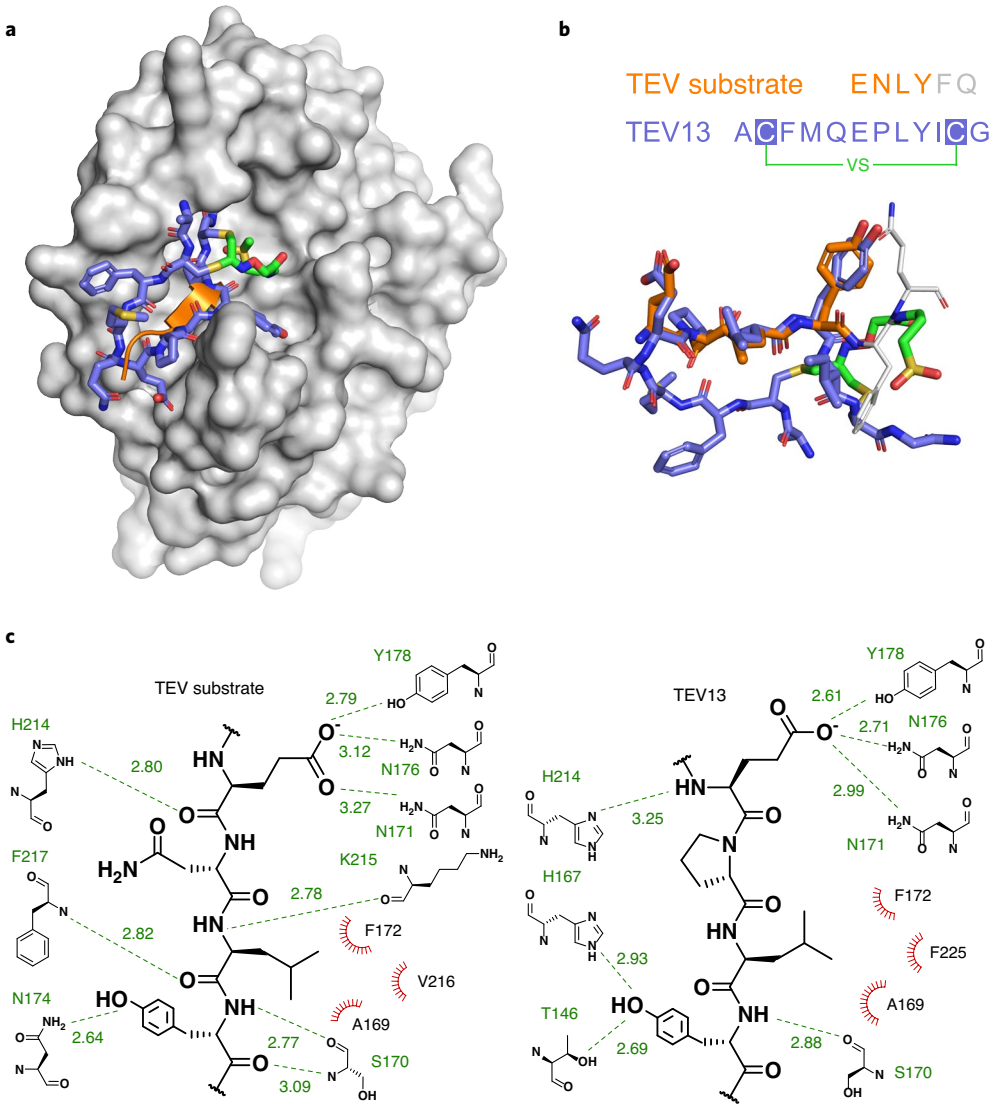


**Fig. 6 | MD simulations to predict the interactions between TEV13 and TEV protease. a**, The MD minimized complex structure of TEV13 (colored in blue) bound to TEV protease (colored in gray). The native substrate of TEV protease is shown as an orange ribbon as found in the reported crystal structure (1LVM). **b**, Structure of the MD-optimized TEV protease-bound TEV13 layered onto the reported X-ray crystal structure of the native peptide substrate ENLYFQ. The key residues P3–P6 that overlap with residues in TEV13 are shown in orange. **c**, Extended diagrammatic representation of interactions between key residues on the native substrate and TEV13 and the active-site region of the TEV protease. Hydrogen-bond interacting partners are shown with green dashed lines, with distance indicated in ångströms. Hydrophobic interactions are depicted as red radiations.

and showed signs of labeling other off-target proteins, as indicated by increased background staining (Fig. 5d and Supplementary Fig. 12). The TEV16 linear probe was as effective at labeling Cat L as the optimized cathepsin probe BMV109 (ref. [31]).

In addition to providing potentially improved target specificity by inducing protein-like folds, the cyclization of peptides also improves overall metabolic stability[9]. We therefore tested the serum stability of the optimal cyclic probe TEV13 and compared it to that of the linear peptide TEV16 and a linear version of the peptide portion of TEV13 in which the two cysteine residues were replaced with serine to prevent disulfide bond formation in the absence of the cyclization linker (Fig. 5e and Supplementary Fig. 13). These data confirmed that both linear peptides were degraded within the first hour, while the cyclic peptide remained fully stable for 1 h and was only partially metabolized over the next 12 h.

**Interactions between cyclic peptide and TEV protease.** To better understand how the optimized cyclic peptide is able to induce selective binding to the TEV protease target, we analyzed this protein–ligand interaction using structural information. We applied molecular dynamics (MD) to simulate the interactions between TEV13 and the TEV protease using the high-resolution structure of TEV protease bound to a six-residue substrate peptide as a template (ENLYF; 1LVM, chain C). While the power of MD calculations for the de novo prediction of ligand–protein interactions can be limited, there are a number of reasons why MD simulations are informative for predicting the interactions between the TEV protease and TEV13. First, the covalent linkage between TEV13 and the TEV protease largely defines the orientation in which the peptide ligand can bind to the target protein, thus greatly narrowing the chemical space to explore and improving the probability of discovering relevant interactions. Second, the critical residues in the cyclic peptide portion of TEV13 are similar to the native TEV substrate sequence of EXLYXQ–S/G (ref. [13]). This allows us to generate a more reliable initial conformation of TEV13. To perform the MD simulations, we covalently linked the VS of TEV13 to the active-site cysteine of TEV

protease to generate input files that were loaded into the Assisted Model Building with Energy Refinement (AMBER) biomolecular simulation package[32]. The complex structure was subjected to MD simulation in explicit TIP3P solvent models with ff14SB and general AMBER force field (GAFF) parameter sets[33,34]. After 40 ns of production simulation, the binding of TEV13 to TEV protease reached a constant and stable status (Supplementary Video 1). The energy of the system remained smooth, and the structure converged to a single low-energy state for the complex (Supplementary Fig. 14). This predicted structure showed TEV13 stably bound to the TEV protease in the primary substrate-binding pocket (Fig. 6a). The side chains of residues E6, L8 and Y9 adopted a conformation similar to that of the native substrate peptide (Fig. 6b). In particular, Y9 in TEV13 matches the positioning of the P3 tyrosine in the TEV substrate peptide, forming a backbone hydrogen bond with S170 and interacting through a hydroxyl group with residues of N174, T146 and H167 that form the S3 pocket of the TEV protease active site (Fig. 6c). Residue L8, which mimics the P4 leucine in the TEV substrate, interacts with F172, V216, F225 and A169. Residue E6 inherited the role of the P6 glutamate by forming several hydrogen bonds with Y178, N176, N171 and H214 located at the lower end of the substrate recognition region. The MD results also indicated that isoleucine at position 10 contributed to the hydrophobic pocket formed by V216 of the TEV protease and L8 of TEV13. This could explain the preference of hydrophobic residues at position 10 of the cyclic peptides. The flexible loop of the cyclic peptide in TEV13 composing residues 3–5 seemed to interact weakly with the N-terminal β-sheet at positions 214–217 of TEV protease, which could explain the relatively narrow structure–activity relationship profile that we observed for residues 3–5. However, the optimized MD structure supports the contribution of cyclization to increased entropy, which enhances binding of TEV13 in the active site. Overall, the MD simulations confirmed that stable and low-energy confirmations can be found in which the cyclic peptide of the TEV13 inhibitor positions the reactive VS for covalent modification by the active-site cysteine residue.

## Discussion

Currently, the most common way to develop new covalent inhibitors involves starting with a potent and selective inhibitor of a target and identifying optimal locations for placement of a reactive functional group and reporter tag. This often requires prior access to a potent lead molecule and a substantial amount of medicinal chemistry efforts. Even when such efforts are successful, in many cases, the resulting compounds still lack absolute specificity for the target. To obtain selectivity over closely related enzymes, it is necessary to test a large diversity of complex ligand scaffolds. Here we demonstrate a phage display method that allows for the screening of libraries of potential covalent inhibitors that number in the billions, resulting in the identification of sequences with high affinity and exceptional selectivity. We reasoned that cyclic peptides, with their rigid, protein-like structures, would have increased potential to direct selectivity of an ABP. Our results for the TEV protease and FphF support this hypothesis.

We chose TEV protease for our initial validation of the phage screening approach because it has a well-defined substrate specificity[13] and there are currently no reported potent and selective inhibitors of this protease. We found that a VS inhibitor containing an optimal linear substrate recognition sequence (TEV16) could in fact inhibit TEV protease. However, this peptide inhibited the lysosomal cysteine Cat L substantially better than the intended target, highlighting the difficulty in generating highly selective covalent inhibitors using short linear peptides. On the other hand, our phage screening efforts identified cyclic peptide sequences that contained some residues that are part of the established substrate-binding region of TEV protease but lack the key P1 glutamine residue that is essential for native substrate recongnition[35]. The resulting cyclic peptide VS compounds only inhibit TEV protease, even though the reactive electrophile can effectively inhibit the other cysteine proteases. These data suggest that we identified conformations that can present key anchor residues to the protease in the absence of key binding interactions of the native substrate and that these extended protein-like binding interactions drive highly selective target binding. MD simulation helped to clarify the binding mode and will direct future efforts to find optimal linkers for use with other enzyme targets.

We chose FphF as a second target for several reasons. First, this enzyme is in a distinct enzyme class from TEV protease and uses a highly conserved α/β-hydrolase domain for hydrolysis with an active-site serine residue. Therefore, we could test the approach using a different enzyme–electrophile pair. Second, we have recently identified a family of Fph hydrolases in *S. aureus* that function as lipid esterases, and at least one of the family members has a role in host colonization[14]. We have performed screening studies using the triazole urea scaffold and found it difficult to identify highly selective inhibitors due to the highly conserved nature of this family[36]. Finally, there is currently no evidence that the DPP electrophile can function as a covalent inhibitor of lipid esterases, thus allowing us to assess the potential of the cyclic peptide to induce covalent bond formation for even suboptimal electrophiles. The result of these efforts is a compound that shows irreversible inhibition of the target hydrolase and a high degree of specificity over the closely related FphB protein. We think this will be particularly valuable because Fph enzymes are expressed in biofilms of *S. aureus* and are therefore potentially valuable targets for imaging agents in vivo. For such imaging agents to be clinically valuable, they must have a high degree of target selectivity.

In summary, we believe that our phage screening approach could be used to find covalently binding ligands for virtually any biomolecule target (protein, glycan, nucleotide, lipid and so on) that contains a slightly reactive nucleophile and the potential to interact with a macromolecular ligand. Our results suggest that the phage approach works well for proteases, but it is likely that the same general linker could be used for screening against other targets that contain a reactive cysteine or serine residue. For example, there have been several recent reports of inhibitors that target cysteine residues in protein kinases[2], and proteomic profiling studies have begun to catalog all potential reactive cysteine residues in a cell[37]. This work has been complemented by other global studies of lysine reactivity, which potentially identifies targets that would be amenable to screening for covalent ligands using this approach[38]. Thus, the covalent phage screening approach could greatly enhance the application of selective covalent ligands in cell biology, imaging and drug development.

## Online content

Any methods, additional references, Nature Research reporting summaries, source data, extended data, supplementary information, acknowledgements, peer review information; details of author contributions and competing interests; and statements of data and code availability are available at https://doi.org/10.1038/s41587-020-0733-7.

Received: 16 September 2019; Accepted: 9 October 2020;
Published online: 16 November 2020

## References

1. Singh, J., Petter, R. C., Baillie, T. A. & Whitty, A. The resurgence of covalent drugs. *Nat. Rev. Drug Discov.* **10**, 307–317 (2011).
2. Ghosh, A. K., Samanta, I., Mondal, A. & Liu, W. R. Covalent inhibition in drug discovery. *ChemMedChem* **14**, 889–906 (2019).
3. Cravatt, B. F., Wright, A. T. & Kozarich, J. W. Activity-based protein profiling: from enzyme chemistry to proteomic chemistry. *Annu. Rev. Biochem.* **77**, 383–414 (2008).

4. Sanman, L. E. & Bogyo, M. Activity-based profiling of proteases. *Annu. Rev. Biochem.* **83**, 249–273 (2014).
5. Cohen, M. S., Zhang, C., Shokat, K. M. & Taunton, J. Structural bioinformatics-based design of selective, irreversible kinase inhibitors. *Science* **308**, 1318–1321 (2005).
6. Smith, G. P. Filamentous fusion phage: novel expression vectors that display cloned antigens on the virion surface. *Science* **228**, 1315–1317 (1985).
7. Matthews, D. J. & Wells, J. A. Substrate phage: selection of protease substrates by monovalent phage display. *Science* **260**, 1113–1117 (1993).
8. Heinis, C., Rutherford, T., Freund, S. & Winter, G. Phage-encoded combinatorial chemical libraries based on bicyclic peptides. *Nat. Chem. Biol.* **5**, 502–507 (2009).
9. Chen, S., Bertoldo, D., Angelini, A., Pojer, F. & Heinis, C. Peptide ligands stabilized by small molecules. *Angew. Chem. Int. Ed. Engl.* **53**, 1602–1606 (2014).
10. Jafari, M. R. et al. Discovery of light-responsive ligands through screening of a light-responsive genetically encoded library. *ACS Chem. Biol.* **9**, 443–450 (2014).
11. Ng, S. & Derda, R. Phage-displayed macrocyclic glycopeptide libraries. *Org. Biomol. Chem.* **14**, 5539–5545 (2016).
12. Cardote, T. A. & Ciulli, A. Cyclic and macrocyclic peptides as chemical tools to recognise protein surfaces and probe protein–protein interactions. *ChemMedChem* **11**, 787–794 (2016).
13. Cesaratto, F., Burrone, O. R. & Petris, G. Tobacco etch virus protease: a shortcut across biotechnologies. *J. Biotechnol.* **231**, 239–249 (2016).
14. Lentz, C. S. et al. Identification of a *S. aureus* virulence factor by activity-based protein profiling (ABPP). *Nat. Chem. Biol.* **14**, 609–617 (2018).
15. Assem, N., Ferreira, D. J., Wolan, D. W. & Dawson, P. E. Acetone-linked peptides: a convergent approach for peptide macrocyclization and labeling. *Angew. Chem. Int. Ed. Engl.* **54**, 8665–8668 (2015).
16. Larsen, D. et al. Exceptionally rapid oxime and hydrazone formation promoted by catalytic amine buffers with low toxicity. *Chem. Sci.* **9**, 5252–5259 (2018).
17. Palmer, J. T., Rasnick, D., Klaus, J. L. & Bromme, D. Vinyl sulfones as mechanism-based cysteine protease inhibitors. *J. Med. Chem.* **38**, 3193–3196 (1995).
18. Oleksyszyn, J., Boduszek, B., Kam, C. M. & Powers, J. C. Novel amidine-containing peptidyl phosphonates as irreversible inhibitors for blood coagulation and related serine proteases. *J. Med. Chem.* **37**, 226–231 (1994).
19. Timmerman, P., Beld, J., Puijk, W. C. & Meloen, R. H. Rapid and quantitative cyclization of multiple peptide loops onto synthetic scaffolds for structural mimicry of protein surfaces. *Chembiochem* **6**, 821–824 (2005).
20. Kather, I., Bippes, C. A. & Schmid, F. X. A stable disulfide-free gene-3-protein of phage fd generated by in vitro evolution. *J. Mol. Biol.* **354**, 666–678 (2005).
21. Chen, S., Morales-Sanfrutos, J., Angelini, A., Cutting, B. & Heinis, C. Structurally diverse cyclisation linkers impose different backbone conformations in bicyclic peptides. *Chembiochem* **13**, 1032–1038 (2012).
22. Hornsby, M. et al. A high through-put platform for recombinant antibodies to folded proteins. *Mol. Cell. Proteom.* **14**, 2833–2847 (2015).
23. Raran-Kurussi, S., Cherry, S., Zhang, D. & Waugh, D. S. Removal of affinity tags with TEV protease. *Methods Mol. Biol.* **1586**, 221–230 (2017).
24. Rebollo, I. R., Angelini, A. & Heinis, C. Phage display libraries of differently sized bicyclic peptides. *MedChemComm* **4**, 145–150 (2013).
25. Nazif, T. & Bogyo, M. Global analysis of proteasomal substrate specificity using positional-scanning libraries of covalent inhibitors. *Proc. Natl Acad. Sci. USA* **98**, 2967–2972 (2001).
26. Albrow, V. E. et al. Development of small molecule inhibitors and probes of human SUMO deconjugating proteases. *Chem. Biol.* **18**, 722–732 (2011).
27. Hemelaar, J. et al. Specific and covalent targeting of conjugating and deconjugating enzymes of ubiquitin-like proteins. *Mol. Cell Biol.* **24**, 84–95 (2004).
28. Choe, Y. et al. Substrate profiling of cysteine proteases using a combinatorial peptide library identifies functionally unique specificities. *J. Biol. Chem.* **281**, 12824–12832 (2006).
29. Bromme, D., Klaus, J. L., Okamoto, K., Rasnick, D. & Palmer, J. T. Peptidyl vinyl sulphones: a new class of potent and selective cysteine protease inhibitors: S2P2 specificity of human cathepsin O2 in comparison with cathepsins S and L. *Biochem. J.* **315**, 85–89 (1996).
30. Sanman, L. E., van der Linden, W. A., Verdoes, M. & Bogyo, M. Bifunctional probes of cathepsin protease activity and pH reveal alterations in endolysosomal pH during bacterial infection. *Cell Chem. Biol.* **23**, 793–804 (2016).
31. Verdoes, M. et al. Improved quenched fluorescent probe for imaging of cysteine cathepsin activity. *J. Am. Chem. Soc.* **135**, 14726–14730 (2013).
32. Salomon-Ferrer, R., Case, D. A. & Walker, R. C. An overview of the Amber biomolecular simulation package. *Wiley Interdiscip. Rev. Comput. Mol. Sci.* **3**, 198–210 (2013).
33. Maier, J. A. et al. ff14SB: improving the accuracy of protein side chain and backbone parameters from ff99SB. *J. Chem. Theory Comput.* **11**, 3696–3713 (2015).
34. Wang, J., Wang, W., Kollman, P. A. & Case, D. A. Automatic atom type and bond type perception in molecular mechanical calculations. *J. Mol. Graph. Model.* **25**, 247–260 (2006).
35. Phan, J. et al. Structural basis for the substrate specificity of tobacco etch virus protease. *J. Biol. Chem.* **277**, 50564–50572 (2002).
36. Chen, L., Keller, L. J., Cordasco, E., Bogyo, M. & Lentz, C. S. Fluorescent triazole urea activity-based probes for the single-cell phenotypic characterization of *Staphylococcus aureus*. *Angew. Chem. Int. Ed. Engl.* **58**, 5643–5647 (2019).
37. Weerapana, E. et al. Quantitative reactivity profiling predicts functional cysteines in proteomes. *Nature* **468**, 790–795 (2010).
38. Hacker, S. M. et al. Global profiling of lysine reactivity and ligandability in the human proteome. *Nat. Chem.* **9**, 1181–1190 (2017).

## Methods

**General synthesis methods.** Chromatographic separations were performed by manual flash chromatography unless otherwise specified. Silica gel 60 (70–230 mesh, Merck) was used for manual column chromatography. Commercial plates (F254, 0.25-mm thickness; Merck) were used for analytical thin-layer chromatography to follow the progress of reactions. Unless otherwise specified, $^{1}$H NMR spectra and $^{13}$C NMR spectra were obtained on a Varian Mercury 400-MHz console connected with an Oxford NMR AS400 actively shielded magnet or a 500-MHz Varian Inova spectrometer at room temperature. Chemical shifts for $^{1}$H or $^{13}$C are given in ppm ($\delta$) relative to tetramethylsilane as an internal standard. Mass spectra ($m/z$) of chemical compounds were recorded on a Finnigan LTQ mass spectrometer (Thermo Scientific), an ACQUITY UPLC SQ Detector 2 system (Waters) or a 1260 Infinity LC (Agilent) connected with an InfinityLab MS detector. Reverse-phase HPLC (RP-HPLC) purifications were performed using a 1260 Infinity HPLC equipped with a semi-prep C18 column (5 µm, C18, 100 Å, 250 × 10 mm liquid chromatography column; Phenomenex) eluted over a linear gradient from 95% solvent A (water and 0.1% trifluoroacetic acid) to 100% solvent B (acetonitrile and 0.1% trifluoroacetic acid).

**Expression of biotinylated TEV protease with AviTag (biotin–TEVp).** During expression, the TEV protease autocleaves the maltose-binding protein moiety, yielding a soluble TEV protease containing a hexahistidine tag for affinity purification and the cleavable biotin tag for releasing covalently bound phage. The biotinylated TEV protease (biotin–TEVp) expression vector pMAL-HisTag-AviTag-3Cs-TEV was built by inserting the AviTag sequence into the pRK793 vector[39]. The TEV protease catalytic domain and vector backbone were amplified by PCR with the following primers: TEV_forward (5′-GTTTTATTCCAGGGTCCTAGTGGT GGCGGTGGAGAAAGCTTGTTTAAGGGGC-3′) and TEV_reverse (5′-ACCTTGAAAATAAAGATTTTCTCCCC-3′). The AviTag sequence was amplified from the pAviTag N-His Kan vector (Ludigen, 49041-1) with primers AviTag-5 (5′-GAGAAAATCTTTATTTTCAAGGT CATCATCACCACCATCACGG-3′) and AviTag-3 (5′-AGGACCCTGGAATAAAACTTCTAAAGAGCCACCGGTAGGAGGAG-3′ ). The two PCR products were then ligated with Gibson Assembly (New England Biolabs, E2611S). The sequence of the final plasmid was verified by Sanger sequencing (MCLAB). The plasmid was transformed into Biotin XCell F′ cells (Lucigen, 49041-1) for expression. An overnight preculture in 5 ml 2YT medium containing 100 µg ml$^{-1}$ carbenicillin was then used for inoculating 500 ml 2YT medium containing 100 µg ml$^{-1}$ carbenicillin and 50 µM biotin on the second day. The cells were cultured at 37 °C until the cell density reached an $OD_{600}$ of 0.4, and then 0.01% arabinose and 1 mM IPTG were added to induce expression of the BirA biotin transferase[40] and the desired TEV protease. Cells were incubated for an additional 4 h at 37 °C, and the expression culture was harvested by centrifugation and lysed in 50 ml of buffer (50 mM Tris 8.0, 100 mM KCl, 1 mM EDTA, 1 mM dithiothreitol (DTT), 0.01% Triton X-100) containing 10 mg lysozyme and 0.5 mg DNase with the help of sonication. After 30 min of incubation on ice, the insoluble cell debris was removed by centrifuging at 10,000$g$ for 20 min. The clarified supernatant was pumped through a HisTrap HP 1-ml column with a peristaltic pump (Rainin Dynamax RP-1) at a flow rate of 1 ml min$^{-1}$. After washing with 50 ml of buffer (50 mM Tris pH 8.0, 100 mM KCl, 1 mM EDTA, 1 mM DTT and 0.01% Triton X-100) containing 10 mM imidazole, the bound protein was eluted over 30 min with an increasing imidazole gradient from 10 mM to 300 mM at a flow rate of 1 ml min$^{-1}$. The eluted protein fractions were combined and concentrated to 5 ml before being injected into a HiPrep 16/60 Sephacryl S-100 HR (GE Healthcare) for purification. The purified fractions of TEV protease were analyzed by SDS–PAGE, and fractions containing the enzyme were combined and stored in 50 mM Tris pH 8.0, 0.5 mM EDTA and 1 mM DTT at −80 °C.

**TEV protease expression.** The TEV protease conjugated with an N-terminal six-histidine tag was expressed in *E. coli* strain BL21(DE3) (Lucigen, 60401-1) using the cytoplasmic expression plasmid pDZ2087 (a gift from D. Waugh). BL21(DE3) cells harboring the plasmid were used to inoculate 5 ml 2YT medium with 100 µg ml$^{-1}$ ampicillin, and on the second day the culture was diluted with 500 ml 2YT medium containing 100 µg ml$^{-1}$ ampicillin for expression. The culture was shaken at 250 r.p.m. at 37 °C until the bacteria reached exponential phase ($OD_{600}$ = 0.5). IPTG (1 mM) was then added to induce the expression of TEV protease. After shaking at 30 °C and 250 r.p.m. for 8 h, the bacteria were harvested by spinning at 8,000 r.p.m. for 15 min. The purification procedure was the same as the one used for purifying biotin–TEVp described above.

**FphF expression and biotinylation.** For the FphF protein (Uniprot accession code Q2FUY3), which is challenging to express and whose function is poorly understood, we chose to use the native, full-length protein (without tag) expressed only with an N-terminal HisTag that could be removed after purification through a 3C protease-cleavable site[41]. This construct produced soluble and catalytically active protein in *E. coli* and was therefore used for the phage panning experiments. Because this protein does not contain the AviTag, we performed chemical biotinylation of free lysine residues. This approach does not allow cleavage at the site of biotinylation, so we constructed a phage library in which a TEV cleavage site was inserted between the N-terminal peptide library and the pIII protein, which allows for the efficient release of covalently bound phage. This approach is a viable alternative to using a target protein that contains a cleavable tag and is optimal for use with targets that do not express well when modified at their C or N termini by the affinity tag. Furthermore, this approach can be used with targets that are hard to express and that can be commercially purchased or purified from native sources (that is, human targets isolated from cells and tissues). In both cases, the presence of a cleavable linker enables stringent washing to remove reversibly bound phage and then subsequent release of the covalently bound phage by cleavage of the linker.

The full-length gene encoding FphF was cloned into a modified pET28a vector encoding a 3C protease cleavage site following the N-terminal six-histidine tag. After transforming the sequence-verified plasmid, FphF was expressed in BL21(DE3) *E. coli* grown in 1 liter LB and induced with 0.2 mM IPTG at 18 °C overnight. Following cell lysis, the cytosolic fraction of the expression host was recovered and mixed with Ni affinity resin to separate crude FphF protein. After washing with purification buffer (50 mM Tris pH 8.0, 300 mM NaCl, 10 mM imidazole, 10% (vol/vol) glycerol and 10% (wt/vol) sucrose), the tagged FphF protein was eluted from the affinity resin with elution buffer (50 mM Tris pH 8.0, 300 mM NaCl, 300 mM imidazole, 10% (vol/vol) glycerol and 10% (wt/vol) sucrose). To remove the N-terminal HisTag, 50 µg ml$^{-1}$ 3C protease and 2 mM DTT were added to the elution buffer and samples were incubated at 4 °C overnight. The final FphF was obtained by sequentially purifying the protein with an ionic exchange RESOURCE Q column and Superdex 75 columns and was stored in buffer (50 mM HEPES pH 7.5 and 100 mM NaCl). For biotinylation, FphF (100 µl at a concentration of 2 mg ml$^{-1}$) was incubated with EZ-link Sulfo-NHS-LC-Biotin (5 µl, 28 mM in DMSO; Pierce) for 2 h on ice. Excess biotinylation reagent was removed by a PD-10 desalting column, and samples were eluted with buffer (50 mM HEPES pH 7.5 and 100 mM NaCl). The biotinylation efficiency was verified by incubating the protein with magnetic streptavidin and neutravidin beads, respectively, and analyzing the bound and unbound protein fraction by SDS–PAGE.

**Peptide–D1D2 fusion protein expression.** A previously reported plasmid[42] (pET28b-C7C-D1D2) was used for expressing a peptide (ACGSGSGSGCG) containing two cysteine residues fused to the phage D1D2 protein (ACGSGSGSGCG–D1D2). The expression and purification procedures were similar to the expression procedure described above except that the following changes were made: BL21(DE3) cells (incubated at 30 °C for 14 h) were used for expression and the final protein was eluted with buffer R (20 mM $NH_4HCO_3$, 5 mM EDTA pH 8.0 with 1 mM TCEP).

**Modification of the peptide–D1D2 fusion protein.** Excess TCEP was removed by exchanging the protein buffer to buffer R without TCEP using a PD-10 column (GE Healthcare). The concentration of the protein was determined using a Nanodrop spectrophotometer based on absorbance at 280 nm. The DCA linker (300 µM) was added to 2 µM fusion protein in buffer R with 20% (vol/vol) acetonitrile and incubated at 30 °C for 2 h or 42 °C for 1 h before being analyzed using an ACQUITY UPLC (Waters) equipped with a C8 column and an SQ Detector 2. The acquired mass of the protein was deconvoluted using MassLynx software.

**DCA–VS linker synthesis.** For a schematic of DCA–VS (**11**) synthesis, see Extended Data Fig. 1.

*tert-Butyl (2,3-dihydroxypropyl)carbamate (**2**).* Triethylamine (4.11 ml, 29.5 mmol) was added dropwise to a solution of 1-aminopropane-2,3-diol (**1**; 23.2 g, 255 mmol) in methanol at room temperature followed by slow addition of a solution of di-*tert*-butyl dicarbonate (66.8 g, 306 mmol) in 200 ml dichloromethane. The reaction mixture was stirred for 3 h at room temperature. After removing the solvent, the oil-like residue was purified using a silica column and eluted with dichloromethane/methanol to yield 40 g of the desired product as an oil (82% yield). $^{1}$H NMR (500 MHz, chloroform-*d*) $\delta$: 5.02 (broad singlet (bs), 1H), 3.89–3.72 (m, 1H), 3.68–3.54 (m, 2H), 3.46–3.17 (m, 2H), 2.81 (bs, 2H), 1.47 (s, 9H).

*tert-Butyl (2-oxoethyl)carbamate (**3**).* Sodium periodate (53.78 g, 251 mmol) was added in portions to a *tert*-butyl (2,3-dihydroxypropyl)carbamate (**2**; 40 g, 209 mmol) solution in 300 ml water. After stirring at room temperature for 2 h, the resulting solids were removed by filtration, and the aqueous fraction was extracted six times with dichloromethane. The combined organic fractions were washed with brine and dried over magnesium sulfate. After filtration, the organic fraction was dried by rotary evaporation and used for the next synthesis step (85% crude yield). $^{1}$H NMR (500 MHz, chloroform-*d*) $\delta$: 9.68 (s, 1H), 5.21 (bs, 1H), 4.10 (d, $J$ = 5.1 Hz, 2H), 1.48 (s, 9H).

*Diethyl ((methylsulfonyl)methyl)phosphonate (**5**).* Fifty percent hydrogen peroxide in water (**4**; 7.4 ml, 260 mmol) was slowly added to a solution of diethyl (methylthio)methylphosphonate (10 g, 50.5 mmol) in acetic acid (34.6 ml, 605 mmol). The reaction mixture was then heated to 70 °C for 30 min. After

removing the solvent by rotary evaporation, the oily residue was diluted with water and extracted six times with dichloromethane. The organic fraction was further washed with saturated sodium bicarbonate in water and brine and dried over anhydrous magnesium sulfate. After filtration, the organic fraction was further dried by rotary evaporation. The resulting white solid was recrystallized in a mixture of ethyl acetate and hexane to give 9.3 g of a colorless crystalline solid (80% yield). $^1$H NMR (500 MHz, chloroform-*d*) $\delta$: 4.57–4.11 (m, 4H), 3.62 (d, $J$ = 16.4 Hz, 2H), 3.24 (s, 3H), 1.41 (t, $J$ = 7.1 Hz, 6H).

*tert-Butyl (E)-(3-(methylsulfonyl)allyl)carbamate (**6**).* In a dry flask under argon, methylmagnesium bromide solution (3 M; 13 ml, 39 mmol) in diethyl ether was added slowly through a syringe to a solution of diethyl ((methylsulfonyl) methyl)phosphonate (**5**; 8.95 g, 38.9 mmol) in dry tetrahydrofuran (100 ml). After stirring at room temperature for 15 min, *tert*-butyl (2-oxoethyl)carbamate (**3**; 6.8 g, 42.8 mmol) solution in dry tetrahydrofuran (100 ml) was slowly added. The solution was then refluxed for 2.5 h. To stop the reaction, 20 ml saturated ammonium chloride solution was added. The product was extracted by washing the aqueous layer three times with 40 ml diethyl ether. After drying with magnesium sulfate, the organic fraction was concentrated, and the crude product was purified using a silica column. The desired product was eluted with hexane and ethyl acetate at a ratio of 3:1 (6.6 g; 72% yield). $^1$H NMR (500 MHz, chloroform-*d*) $\delta$: 6.94 (dt, $J$ = 15.7, 4.8 Hz, 1H), 5.97 (dt, $J$ = 15.8, 1.9 Hz, 1H), 4.73 (s, 1H), 3.95 (t, $J$ = 5.6 Hz, 2H), 3.76 (s, 3H), 1.48 (s, 9H). $^{13}$C NMR (126 MHz, chloroform-*d*) $\delta$: 166.55, 145.26, 120.71, 79.73, 60.37, 51.58, 41.28 and 28.30.

*tert-Butyl (E)-(2-((3-(methylsulfonyl)allyl)amino)-2-oxoethoxy)carbamate (**9**).* A solution of *tert*-butyl (*E*)-(3-(methylsulfonyl)allyl)carbamate (**6**; 80 mg, 0.34 mmol) in 50% trifluoroacetic acid with dichloromethane was stirred at room temperature for 1 h before the solvent was removed under vacuum, and toluene was added twice to co-evaporate the trifluoroacetic acid. The remaining oily residue was triturated with diethyl ether to produce a brownish solid (50 mg, 0.216 mmol). Then, 2-(((*tert*-butoxycarbonyl)amino)oxy)acetic acid (**8**; 50 mg, 0.262 mmol) was added followed by *N*,*N*′-diisopropylcarbodiimide (27.2 mg, 0.216 mmol) and *N*,*N*-diisopropylethylamine (38 µl, 0.218 mmol). After stirring at room temperature overnight, the insoluble solids were filtered off, and the dichloromethane fraction was purified directly by silica chromatography to produce 42 mg of product for a 63% yield. $^1$H NMR (500 MHz, chloroform-*d*) $\delta$: 8.68 (bs, 1H), 7.81 (s, 1H), 6.92 (dt, $J$ = 15.2, 4.3 Hz, 1H), 6.55 (dt, $J$ = 15.2, 2.0 Hz, 1H), 4.37 (s, 2H), 4.18 (ddd, $J$ = 6.2, 4.3, 2.0 Hz, 2H), 2.93 (s, 3H), 1.47 (s, 9H). $^{13}$C NMR (126 MHz, chloroform-*d*) $\delta$: 169.32, 158.18, 143.91, 129.88, 105.00, 83.69, 42.84, 38.88 and 28.06.

*(E)-2-(((1,3-dichloropropan-2-ylidene)amino)oxy)-N-(3-(methylsulfonyl)allyl) acetamide (DCA–VS; **11**).* *tert*-Butyl (*E*)-(2-((3-(methylsulfonyl)allyl)amino)-2-oxoethoxy)carbamate (**10**; 42 mg, 0.136 mmol) was placed in 1 ml of a 50% trifluoroacetic acid solution in dichloromethane at room temperature for 1 h. The solvent was removed under vacuum. Toluene was added and dried twice to remove the residual trifluoroacetic acid. The resulting alkoxyl amine was mixed with 1,3-dichloroacetone (25 mg, 0.198 mmol) in 1 ml of dimethylformamide. The mixture was stirred at room temperature overnight. After removing dimethylformamide, the residue was purified by silica chromatography and the desired product was eluted with 3% methanol in dichloromethane to produce 26 mg product for a 60% yield. $^1$H NMR (400 MHz, chloroform-*d*) $\delta$: 8.01 (s, 1H), 6.90 (dt, $J$ = 15.2, 4.4 Hz, 1H), 6.46 (d, $J$ = 15.2 Hz, 1H), 4.71 (s, 2H), 4.35 (s, 2H), 4.27 (s, 2H), 4.19 (ddd, $J$ = 6.4, 4.5, 1.9 Hz, 2H), 2.94 (s, 3H). $^{13}$C NMR (101 MHz, chloroform-*d*) $\delta$: 168.98, 154.30, 143.64, 130.22, 73.65, 42.84, 41.78, 38.84, 32.79. MS (electrospray ionization (ESI)): calculated for $C_9H_{15}Cl_2N_2O_4S^+$: 317.0; found: 317.0.

**DCA–DPP linker synthesis.** For a schematic of DCA–DPP (**15**) synthesis, see Extended Data Fig. 2.

*Benzyl ((diphenoxyphosphoryl)methyl)carbamate (**13**).* A mixture of benzyl carbamate (6.04 g, 40 mmol), acetic anhydride (**12**; 5.18 g, 51 mmol) and paraformaldehyde (1.22 g, 40 mmol) in 40 ml acetic acid was heated to 70 °C for 3 h. Triphenyl phosphite (12.4 g, 40 mmol) was then added and the mixture was heated at 120 °C for 2 h. The volatile components were removed in vacuo, and the residue was dissolved in methanol and left overnight at −20 °C. The precipitate was isolated via filtration, washed with cold methanol and dried at room temperature to yield **13** as a white solid (46%). $^1$H NMR (400 MHz, chloroform-*d*) $\delta$: 7.48–7.02 (m, 15H), 5.46 (s, 1H, NH), 5.13 (s, 2H), 4.04–3.92 (m, 2H). MS (ESI): calculated for $C_{21}H_{21}NO_5P^+$: 398.1; found: 398.1.

*tert-Butyl (2-(((diphenoxyphosphoryl)methyl)amino)-2-oxoethoxy)carbamate (**14**).* The benzyl ((diphenoxyphosphoryl)methyl)carbamate (**13**; 2.22 g, 5.60 mmol) product was treated with 33% hydrogen bromide/acetic acid (10 ml), and the reaction mixture was stirred for 2 h. After 2 h, the reaction mixture was concentrated, and the residue was dissolved in diethyl ether and left overnight at −20 °C. The resulting white precipitate was filtered, washed with cold diethyl ether and dried at room temperature. Directly to the precipitate was added (Boc-aminooxy)acetic acid (1.13 g, 6.71 mmol), *N*,*N*′-diisopropylcarbodiimide (865 µl, 5.60 mmol) and *N*,*N*-diisopropylethylamine (1.95 ml, 11.20 mmol) in 20 ml dimethylformamide, and the reaction mixture was stirred overnight at room temperature. The reaction mixture was concentrated, and the residue was purified by flash silica chromatography using a gradient of 10–100% ethyl acetate in hexane. After concentration of pure fractions, **14** was obtained as a white solid (67% yield). $^1$H NMR (400 MHz, DMSO-*d6*) $\delta$: 7.48–7.35 (m, 4H), 7.31–7.15 (m, 6H), 4.30 (d, $J$ = 1.3 Hz, 2H), 4.09 (dd, $J$ = 10.9, 6.0 Hz, 2H), 1.40 (s, 9H). MS (ESI): calculated for $C_{20}H_{25}N_2O_7P^+$: 436.1; found: 436.1.

*Diphenyl ((2-(((1,3-dichloropropan-2-ylidene)amino)oxy)acetamido)methyl) phosphonate (**15**).* *tert*-Butyl (2-(((diphenoxyphosphoryl)methyl)amino)-2-oxoethoxy)carbamate (**14**; 1 g, 2.30 mmol) was dissolved in 10 ml of 50% trifluoroacetic acid in dichloromethane and stirred at room temperature for 1 h. The reaction mixture was concentrated, and the resulting alkoxyl amine was mixed with 1,3,-dichloroacetone (0.43 g, 3.45 mmol) in 1 ml of dimethylformamide overnight at room temperature. The reaction mixture was concentrated, and the residue was purified by flash silica chromatography using a gradient of 0–10% methanol in dichloromethane. After concentration of pure fractions, **15** was obtained as a white solid in 72% yield. $^1$H NMR (400 MHz, chloroform-*d*) $\delta$: 7.39–7.32 (m, 4H), 7.25–7.17 (m, 6H), 6.70 (t, $J$ = 4.3 Hz, 1H), 4.71 (d, $J$ = 1.4 Hz, 2H), 4.33 (s, 2H), 4.20 (s, 2H), 4.16 (s, 1H). $^{13}$C NMR (101 MHz, chloroform-*d*) $\delta$: 168.71 (s), 168.65 (s), 154.19 (s), 149.91 (s), 149.83 (s), 129.93 (s), 125.68 (s), 120.56 (s), 120.49 (s), 73.64 (s), 41.70 (s), 35.55 (s), 33.97 (s), 32.61 (s). $^{31}$P NMR (162 MHz, chloroform-*d*) $\delta$: 14.71 (s). MS (ESI): calculated for $C_{18}H_{19}Cl_2N_2O_5P^+$: 444.0; found: 444.0.

**Glutamine–VS warhead synthesis.** For a schematic of the synthesis of glutamine–VS peptides, see Extended Data Fig. 3.

*9-Fluorenylmethoxycarbonyl (Fmoc)-Glu(OtBu)-dimethyl hydroxyl (Weinreb) amide (**16**).* Fmoc-Glu(OtBu)-OH (10.34 g, 24.3 mmol), hydroxybenzotriazole (3.6 g, 26.7 mmol) and dicyclohexylcarbodiimide (5.5 g, 26.7 mmol) were dissolved in 50 ml dimethylformamide. After stirring for 30 min at room temperature, a solid formed and was removed by filtration. *N*,*O*-dimethyl hydroxyl amine (2.84 g, 29.2 mmol) was added to the filtered reaction mixture along with triethylamine (2.94 g, 29.2 mmol). The reaction was stirred for an additional 12 h and then concentrated. The crude oil was then dissolved in ethyl acetate and washed with three portions each of saturated sodium bicarbonate, 0.1 N HCl and brine. The organic layer was dried over magnesium sulfate and concentrated to dryness. This crude preparation was used in subsequent reactions without further purification. $^1$H NMR (400 MHz, chloroform-*d*) $\delta$: 7.76 (d, $J$ = 7.4 Hz, 2H), 7.64–7.56 (m, 2H), 7.40 (t, $J$ = 7.4 Hz, 2H), 7.36–7.27 (m, 2H), 5.60 (d, $J$ = 8.8 Hz, 1H), 4.36 (d, $J$ = 7.3 Hz, 2H), 4.21 (t, $J$ = 7.2 Hz, 1H), 3.78 (s, 3H), 3.21 (s, 3H), 2.38–2.29 (m, 2H), 2.16–1.81 (m, 2H), 1.44 (s, 9H).

*Fmoc-Glu(OtBu)-H (**17**).* Crude **16** (11 g, 23.5 mmol) was dissolved in anhydrous ethyl ether and stirred on ice under a positive argon flow. Lithium aluminum hydride (0.891 g, 23.5 mmol) was slowly added, leading to gas evolution. The reaction was stirred for an additional 20 min and then quenched by the addition of potassium hydrogen sulfate (6.67 g, 49 mmol). The quenched reaction was stirred on ice for 20 min and then at room temperature for an additional 30 min. The mixture was extracted three times with ethyl acetate, and the combined organics were washed with three portions of 0.1 M HCl, saturated sodium carbonate and brine. The organic phase was concentrated to an oil. The product was purified by flash chromatography in hexanes:ethyl acetate (2:1 (vol/vol)). Yield (1 g, 10.4%). $^1$H NMR (400 MHz, chloroform-*d*) $\delta$: 9.59 (s, 1H), 7.77 (d, $J$ = 7.8 Hz, 2H), 7.60 (d, $J$ = 7.5 Hz, 2H), 7.41 (t, $J$ = 7.5 Hz, 2H), 7.32 (t, $J$ = 7.5 Hz, 2H), 5.61–5.51 (m, 1H), 4.50–4.38 (m, 2H), 4.22 (t, 1H), 2.44–2.28 (m, 2H), 1.98–1.85 (m, 2H), 1.44 (s, 9H).

*Fmoc-Glu(OtBu)-VS (**18**).* Diethyl (methylthiomethyl) phosphonate was oxidized to the corresponding phosphonate sulfone using hydrogen peroxide in acetic acid as described above for **5**. Diethyl phosphonate sulfone (96 mg, 0.417 mmol) was dissolved in anhydrous tetrahydrofuran under argon. Methylmagnesium bromide solution (3 M; 139 µl, 0.417 mmol) in diethyl ether was added, and the reaction was stirred for 30 min at room temperature. Pure **17** (170 mg, 0.416 mmol) was dissolved in anhydrous tetrahydrofuran under argon and added to the stirring reaction by syringe. After 30 min of stirring at room temperature, the reaction was quenched with water, and the aqueous phase was washed three times with dichloromethane. The organic phases were combined, dried over $MgSO_4$ and evaporated to dryness. The crude oil was purified by flash chromatography over silica gel in hexane:ethyl acetate (1.5:1 (vol/vol)). Yield (168 mg, 8.7 mmol, 34.6%). $^1$H NMR (500 MHz, chloroform-*d*) $\delta$: 7.81 (d, $J$ = 7.5 Hz, 2H), 7.62 (s, 2H), 7.48–7.41 (m, 2H), 7.40–7.34 (m, 2H), 6.84 (dd, $J$ = 14.6, 4.9 Hz, 1H), 6.46 (d, $J$ = 15.0 Hz, 1H), 5.26 (d, $J$ = 8.0 Hz, 1H), 4.49 (d, $J$ = 6.3 Hz, 2H), 4.23 (t, $J$ = 6.7 Hz, 1H), 2.96 (s, 3H), 2.46–2.28 (m, 2H), 2.04–1.83 (m, 2H), 1.48 (s, 9H).

*Fmoc-Glu(Rink amide resin)-VS (**19**).* Pure **18** (17 mg, 35 µmol) was dissolved in methylene chloride (0.5 ml), and an equal volume of anhydrous trifluoroacetic acid was added. After 1 h of stirring at room temperature, an equal volume of toluene

was added, and the reaction mixture was concentrated by rotary evaporation. The crude product was then coupled to Rink amide resin (60 mg, 0.35 mmol $g^{-1}$ load, 21 µmol) in dimethylformamide (1 ml) using HATU (13.3 mg, 35 µmol) and *N*,*N*-diisopropylethylamine (11 µl, 105 µmol) for 2 h at room temperature. The resin was washed with dimethylformamide, and peptide chain extension was achieved with standard solid-phase peptide synthesis.

**Construction of a phage peptide library with a TEV protease cutting site.** Insertion of the TEV cleavage site sequence did not reduce the production yield or infectivity of the phage library (data not shown). The phage library was created by inserting DNA sequences encoding semi-random peptide sequences ($AXCX_2C$), the linker GGSG, the TEV protease-cleavable peptide ENLYFQSG and the disulfide-free domains D1 and D2 into the phage fdg3p0ss vector[20], resulting in the generation of a library with $8 \times 10^8$ diversity. The insert was generated in two consecutive PCR reactions. First, the genes encoding the TEV protease peptide and D1 and D2 of the phage pIII protein were PCR amplified with primers SecPCRba (5′-TGTGGCGGTTCTGGCGCTC-3′) and sfi2notfo (5′-CCATGGCCCCCGAGGCCGCGGCCGCATTGACAGG-3′) using the vector fdg3p0ss21 as a template. Second, the DNA encoding the random peptides was appended in a PCR reaction using the following primers: C7C_lib_F ( 5′-TATGCGGCCCAGCCGGCCATGGCANNKTGTNN KNNKNNKNNKNNKNNKNNKTGTGGCGGTTCTGGCGCTC-3′) and sfi2notfo. The PCR products were digested with SfiI and ligated into an SfiI-digested phage vector. After verifying the efficiency of ligation, the library plasmids were electroporated into *E. coli* TG1 cells and cells were incubated for 1 h in 2YT medium at 37 °C. The phage library was then amplified by plating onto large (20 cm in diameter) chloramphenicol (30 mg $ml^{-1}$) 2YT plates. After growing at 37 °C overnight for 16 h, colonies were scraped off the plates with 2YT medium supplemented with 10% (vol/vol) glycerol and stored at −80 °C.

**Phage panning.** Phage harboring the cysteine-rich peptide library ($CX_8C$; a generous gift from C. Heinis (EPFL)) were used for selecting peptides against the TEV protease. The randomized DNA sequences encoding the peptide library were inserted into the phage DNA between the pelB signal peptide and the disulfide-free pIII protein of the fdg3p0ss phage vector[20]. The phage peptide library bearing a TEV protease-cleavable site was used for selection of peptides against FphF hydrolase. To overcome the low infectivity of the disulfide-free phage strain used in our screens, we used a large volume of 2YT rich medium (1 liter) for the production of phage. The phage peptide libraries in TG1 *E. coli* bacteria (Lucigen, 60502-1) were thawed from stock and used for inoculating 2YT medium containing 30 µg $ml^{-1}$ chloramphenicol. Phage were generated by incubating at 30 °C with shaking at 250 r.p.m. for 16 h. On the second day, the medium rich with secreted phage was separated from the host bacteria by spinning at 8,500 r.p.m. for 30 min, and the supernatant was mixed with 250 ml of a solution containing 20% polyethylene glycol 6000 and 2.5 M NaCl. Following a 1-h incubation on ice, the precipitated phage were spun at 9,000 r.p.m. for 45 min. The resulting phage pellet was then dissolved in 10 ml buffer R (20 mM ammonium bicarbonate pH 8.0 and 5 mM EDTA) and reduced with 1 mM TCEP at 42 °C for 1 h. After removing the excess TCEP by filtration, 16 ml buffer R was added and 4 ml linker (DCA–VS; 1.5 mM) in acetonitrile was added to modify the phage at 30 °C for 2 h. Then, 5 ml of a solution with 20% polyethylene glycol 6000 and 2.5 M NaCl was added to precipitate the phage, and the recovered phage pellets were resuspended in TEV buffer (50 mM Tris pH 8.0, 100 mM KCl, 1 mM EDTA and 1 mM DDT) for selections against TEV protease or FphF buffer (50 mM HEPES pH 7.5 and 100 mM NaCl) for selections against FphF hydrolase; both were supplemented with 1% BSA and 0.1% Triton X-100 for blocking at room temperature for 0.5 h. Biotin–TEV protease or FphF–biotin (10 µg) was incubated with 50 µl of hydrophilic streptavidin magnetic beads (New England Biolabs, S1421S) for 0.5 h, and beads were washed five times with TEV buffer supplemented with 1% BSA and 0.1% Triton X-100. After being blocked in the same buffer for 0.5 h, the phage library was mixed with the magnetic beads and incubated at room temperature for different amounts of time depending on the round of screening being performed. After washing ten times with PBS, the magnetic beads were incubated with 100 µl guanidine chloride in PBS for 5 min, and then each was eluted with 10 µM TEV protease in 300 µl TEV buffer (50 mM Tris pH 8.0, 0.5 mM EDTA and 1 mM DTT) at 34 °C for 1 h to release the covalently bound phage from the solid support. The released phage were used to infect 45 ml of TG1 bacteria at an $OD_{600}$ of 0.4 for 1.5 h in a 37 °C incubator without shaking. Afterwards, the TG1 cells were pelleted at 3,000 r.p.m. for 15 min and plated on two 15-cm 2YT agar plates with 30 µg $ml^{-1}$ chloramphenicol antibiotic for each protease. The agar plate was then incubated at 37 °C overnight to allow the infected TG1 cells to expand. On the second day, TG1 cells were scraped off the agar plates with 5 ml 2YT medium, mixed with 5 ml 50% glycerol and stored at −80 °C. This glycerol stock was then used for preparing plasmids for sequencing or for generating phage for the next round of phage panning.

**Phage infectivity measurement.** Phage stock solution (5 µl) was added to 1 ml PBS containing 0, 1, 2, 3, 4, 5 and 6 M guanidine chloride and incubated at room temperature for 5 min. Phage stock solution (5 µl) was added to 1 ml of TEV buffer containing 0–25 ng $ml^{-1}$ TEV protease and incubated at room temperature for 0.5 h. Each solution was serially diluted 12 times by taking 20 µl of sample and adding it to 180 µl of 2YT medium. Each dilution (20 µl) was added to 180 µl of exponentially growing TG1 cells ($OD_{600} = 0.4$) and incubated for 90 min at 37 °C. Ten microliters of the infected TG1 cells was then spotted onto 2YT agar plates containing 30 µg $ml^{-1}$ chloramphenicol. The number of colonies was counted the next day, and the number of infective phage was calculated.

**Peptide modification.** All peptides were prepared using standard solid-phase peptide synthesis on a Syro II automated parallel peptide synthesizer (Biotage) using standard Fmoc chemistry protocols and Rink Amide AM resin support (0.02-mmol scale). Fmoc groups were removed using 300 µl of a 20% (vol/vol) solution of piperidine in dimethylformamide, and amino acid coupling was carried out using a double coupling strategy with a fourfold excess of Fmoc-labeled amino acids (0.5 M solution in dimethylformamide). Coupling was achieved using a 1:1:1.5 ratio of amino acid:HBTU:*N*,*N*-diisopropylethylamine in dimethylformamide. The deprotection and coupling times were 5 and 30 min, respectively. Six washes with 600 µl dimethylformamide were performed between deprotection and coupling steps. The peptide-loaded resin was treated with cleavage cocktail K (90:2.5:2.5:2.5:2.5 (vol/vol) mixture of trifluoroacetic acid:thioanisole:water:phenol:1,2-ethanedithiol) for 2 h, which simultaneously cleaved the peptide from the resin and removed all side chain-protecting groups. The cleaved peptides were subsequently isolated by precipitation in cold diethyl ether followed by centrifugation. The precipitated peptides were resuspended in diethyl ether and centrifuged three times. Finally, the peptides were dissolved in degassed MilliQ water and lyophilized[43]. To perform peptide cyclization, 10 mg of the crude peptide was dissolved in 9 ml degassed solvent mixture of 20% acetonitrile and 80% water, resulting in a peptide concentration of about 1 mM, followed by the addition of 3.5 mg DCA–VS or DCA–DPP linker in 0.5 ml acetonitrile and 0.5 ml of 1 M $NH_4HCO_3$ in water. After incubation at 30 °C for 1 h, the reaction mixture was quenched with 50 µl trifluoroacetic acid and lyophilized to dryness. For purification, the modified peptides were dissolved in 400 µl water and injected onto a 1260 Infinity HPLC (Agilent) equipped with a semi-prep C18 column (5 µm C18, 100 Å, 250 × 10 mm liquid chromatography column; Phenomenex) and separated over a linear gradient from 95% solvent A (water and 0.1% trifluoroacetic acid) to 100% solvent B (acetonitrile and 0.1% trifluoroacetic acid) in 15 min. The mass of peptides was measured using a Bruker MALDI microflex LRF. HPLC fractions were lyophilized, and resulting solids were dissolved in DMSO to a stock concentration of 10 mM and stored at −20 °C.

**Fluorogenic substrate synthesis.** The TEV substrate peptide (ENLYFQGK, 20 µmol) was synthesized by standard Fmoc-based solid-phase peptide synthesis on Rink Amide resin (0.33 mmol $g^{-1}$ load; Chem-Impex International, 02900) as described above. After deprotecting the Fmoc from the N terminus of the synthesized peptide, Cy5 acid (14 mg, 22 µmol), HATU (12 mg, 31.5 µmol) and *N*,*N*-diisopropylethylamine (18 µl, 103 µmol) were added to the washed resin and incubated for 2 h at room temperature. After releasing and deprotecting the peptide with cleavage cocktail K, the Cy5-labeled peptide was purified by HPLC and lyophilized to dryness. MS (ESI) negative: calculated for $M\text{-}H^+$: 1,620.7; found: 1,620.4. Cy5-ENLYFQGK-$NH_2$ (10 mg, 6.2 µmol), QSY21 (7 mg, 7.5 µmol) and *N*,*N*-diisopropylethylamine (6.5 µl, 37.4 µmol) were mixed in 1 ml DMSO and incubated at room temperature overnight. The reaction mixture was injected into an RP-HPLC connected with a semi-prep C18 column to purify Cy5-ENLYFQGK(QSY21)-$NH_2$ as described above. MS (ESI) negative: calculated for $M\text{-}2H^+$: 1,221.4; found: 1,221.4.

**TEV protease inhibition assay.** The inhibitory activity of cyclic peptides was determined by incubating TEV protease (50 nM) with different concentrations of inhibitor and quantifying residual activity using the fluorogenic substrate synthesized as described above (50 µM, Cy5-ENLYFQGK(QSY21)-$NH_2$). Peptide inhibitors and TEV protease were preincubated at 30 °C for 1 h, and then the enzymatic assays were performed at 30 °C in buffer containing 50 mM Tris-Cl pH 8.0, 100 mM KCl, 1 mM EDTA, 1 mM DTT, 1% DMSO, 1% BSA and 0.01% Triton X-100. TEV activity was measured by monitoring the change in fluorescence intensity during 1 h using a Cytation 3 Multi-Mode Reader (excitation, 640 nm; emission, 670 nm; BioTek Instruments). Calculations were done with OriginPro 2019 software (OriginLab Corporation). Sigmoidal curves were fitted to the data using the following dose–response equation: $y = A1 + (A2 - A1)/(1 + 10^{\log(IC_{50} - x)p})$ ($x$, peptide concentration; $y$, percent activity of the reaction without peptide; A1, 100%, $y$ value at the top plateau; A2, 0%, $y$ value at the bottom plateau; $p$, 1, Hill coefficient). $IC_{50}$ values were derived from the fitted curve.

**Synthesis of the SENP1 substrate Ac-QTGG-7-amino-4-trifluoromethylcoumarin.** $POCl_3$ (400 µl, 4.29 mmol) was slowly added to a solution of 7-amino-4-trifluoromethylcoumarin (AFC; 500 mg, 2.18 mmol) and Boc-G-OH (381 mg, 2.18 mmol) in pyridine (10 ml) at −15 °C under argon, and the resulting mixture was further stirred at −15 °C for 0.5 h. The reaction was then quenched with water and extracted with ethyl acetate. The organic phase

was combined and washed with 0.1 M HCl, water and brine. After drying over magnesium sulfate, the organic phase was concentrated, and the resulting crude material was purified by silica column to afford Boc-G-AFC as a white solid (630 mg, 74% yield). After Boc deprotection with a mixture of trifluoroacetic acid and dichloromethane (1:1, 10 ml) at room temperature for 1 h, the reaction mixture was dried and injected into a CombiFlash Companion Flash Chromatography System equipped with a RediSep Rf reversed-phase C18 column (Teledyne) for purification. $H_2$N-G-AFC was isolated as a white solid (550 mg, 88%). MS (ESI): calculated for M+H$^+$: 287.2; found: 287.1.

Ac-Q(trt)T(t-Bu)G-OH (Ac, acetyl) was synthesized on chlorotrityl resin as described above and cleaved with 20% hexafluoroisopropanol in dichloromethane 3×5 min to keep the peptide fully protected. MS (ESI): calculated for M+H$^+$: 645.3; found: 644.9. Ac-Q(trt)T(t-Bu)G-OH, $H_2$N-G-AFC, *N*,*N*′-diisopropylcarbodiimide and *N*,*N*-diisopropylethylamine were mixed in dichloromethane and stirred at room temperature overnight. The next morning, the generated white solid was removed by filtration, and the reaction mixture was dried under vacuum and deprotected with 1 ml trifluoroacetic acid:triisopropylsilane:water (95:2.3:2.5) for 2 h at room temperature. After removing the solvent, the residue was dissolved in DMSO and purified by HPLC. Fractions with the correct MS were combined and lyophilized to give a white solid. MS (ESI): calculated for M+H$^+$: 615.2; found: 615.3.

**FphF inhibitory activity test.** FphF peptides were tested in a similar manner to TEV peptides with the following changes: all assays were performed in FphF buffer (20 mM HEPES pH 7.5, 50 mM NaCl, 0.01% Triton X-100 and 5% DMSO) with final concentrations of 1 nM FphF and 20 μM 4-MU heptanoate. FphF without any inhibitor was used as a positive control, and substrate in buffer without enzyme was taken as a negative control. Peptides were preincubated for 1 h at 37 °C before residual FphF activity was determined.

**Cat S, Cat L, SENP1, FphB and trypsin inhibition.** The inhibitory activity of peptides against Cat S, Cat L, SENP1 (ref. [44]), FphB[14] and trypsin was determined by preincubating peptide inhibitors with proteases and quantifying residual activity with a fluorogenic substrate in the same procedure as described for determining TEV inhibition activities. For Cat S and Cat L inhibition, a final concentration of 2–200 μM peptide was preincubated with 2.5 nM Cat S or Cat L enzyme at 37 °C for 1 h before 100 μM Z-FR-AMC (Z, N-carbobenzyloxy; AMC, 7-amino-4-methylcoumarin) substrate was added in buffer containing 100 mM sodium acetate, 2.5 mM EDTA, 2.5 mM DTT, 0.01% Tween-20 and 1% DMSO. Monitoring the generation of free AMC due to hydrolysis of the fluorogenic substrate was achieved by reading fluorescent signal (excitation, 380 nm; emission, 460 nm). For SENP1 inhibition, final concentrations of 2–200 μM of peptide were preincubated with 500 nM SENP1 enzyme at 37 °C for 1 h before 100 μM Ac-QTGG-AFC (AFC, 7-amino-4-trifluoromethylcoumarin) substrate was added in buffer containing 50 mM Tris pH 7.5, 100 mM NaCl, 1 mM EDTA, 1 mM DTT, 5% DMSO and 0.01% Tween-20. Monitoring the generation of free AMC due to the hydrolysis of fluorogenic substrate was achieved by reading fluorescent signals (excitation, 400 nm; emission, 505 nm). For the FphB inhibition assay, a final concentration of 0.5–50 μM peptide was preincubated with 200 nM FphB enzyme at 37 °C for 1 h before 20 μM 4-MU butyrate substrate was added in PBS. Monitoring the generation of free 4-methylumbelliferone due to hydrolysis of fluorogenic substrate was achieved by reading fluorescent signals (excitation, 380 nm; emission, 460 nm). For the trypsin inhibition assay, a final concentration of 0.5–50 μM peptide was preincubated with 20 μg ml$^{-1}$ trypsin enzyme at 37 °C for 1 h before 50 ng FITC-casein substrate was added in 100 mM Tris 8.5 buffer. Monitoring the generation of free FITC due to hydrolysis of fluorogenic substrate was achieved by reading the fluorescent signal (excitation, 490 nm; emission, 525 nm). The slope of the developing curve reflected the residual activity of enzymes after covalent inhibition. The $IC_{50}$ values were calculated as described above.

**Determination of $k_{inact}/K_i$.** Under pseudo-first-order conditions using the same buffers as outlined above, a fixed amount of TEV protease (50 nM) or FphF (100 nM) was incubated with TEV13 or FphF16, respectively, at different concentrations in the presence of the appropriate substrate (50 μM Cy5-ENLYFQGK(QSY21)-$NH_2$ for TEV and 20 μM 4-MU heptanoate for FphF). The pseudo-first-order rate constant, $k_{obs}$, was calculated for each inhibitor concentration using nonlinear regression analysis in GraphPad Prism 5. The obtained values were plotted against inhibitor concentration to afford the apparent second-order rate constant $k_{inact}/K_i$.

**Cy5-labeled TEV13 peptide.** Cy5-NHS (1 mg, 1.35 μmol) and *N*,*N*-diisopropylethylamine (1 μl, 5.75 μmol) were added to a solution of the TEV13 peptide (10 mM, 50 μl) in DMSO. The reaction mixture was incubated at room temperature overnight and injected into the HPLC instrument for purification as described above. The fractions with the desired product were combined and lyophilized to dryness. MS (MALDI): calculated for M+H$^+$: 2,276.8; found: 2,276.5.

**Labeling with Cy5–TEV13-DCA–VS.** HEK293 cells from ATCC were cultured in DMEM (Gibco, 11995-073) supplemented with antibiotics (Gibco, 15140148) and 10% FBS (GeneMate, S-1200-500); no mycoplasma testing was performed. One 10-cm Petri dish of HEK293 cells or TG1 *E. coli* grown in 5 ml 2YT medium was individually resuspended in 1 ml TEV buffer (50 mM Tris pH 8, 100 mM KCl, 1 mM EDTA and 1 mM DTT) with 0.2% Triton X-100. The cells were transferred to 2-ml O-ring tubes and mixed with 100 μl of 0.1-mm glass beads (Biospec Products). Tubes were then placed in a prechilled aluminum vial rack, and cell samples were lysed in a Mini-Beadbeater-96 (Biospec Products) three times (30 s with 2 min resting on ice in between). After centrifugation at 13,000*g* at 4 °C for 5 min, 50 μl of the cleared supernatant was mixed with 50 μl TEV buffer with or without 100 nM TEV protease for labeling with 1 μM Cy5–TEV13-DCA–VS at 30 °C for 1 h. Then, 40 μl SDS–PAGE loading buffer was added, and the mixtures were heated to 95 °C for 5 min. Samples from each condition (15 μl) were separated by 12% SDS–PAGE. Cy5 fluorescence was detected by scanning on a Typhoon 9410 Variable Mode Imager ($\lambda_{ex}$ = 633 nm, 670 BP30 filter; GE Healthcare)[45]. The fluorescence intensity of labeled proteins was analyzed with LI-COR Image Studio Lite software and plotted with OriginPro 2019 software (OriginLab Corporation). Afterwards, the gel was stained with Coomassie blue to visualize total protein.

**Ellman's test of free cysteine in TEV13.** Free cysteine solutions (0.5 μl of 2, 4, 6, 8 and 10 mM) in buffer D (0.1 M sodium phosphate pH 8.0 and 1 mM EDTA) were mixed with 9.5 μl buffer D and 10 μl DTNB (80 μg ml$^{-1}$) and incubated at room temperature for 15 min. Three replicates of each condition were obtained. The absorbance at 412 nm was measured using a UV spectrophotometer to generate a standard curve. Cyclic peptide TEV13 was dissolved in DMSO to achieve a stock concentration of 10 mM. The stock solution (0.5 μl) was mixed with 9.5 μl buffer D and 10 μl DTNB (80 μg ml$^{-1}$) and incubated at room temperature for 15 min. The absorbance at 412 nm was measured using a UV spectrophotometer and fit to the standard curve generated with free cysteine[46].

**Competition of TEV13 for labeling by Cy5–TEV13.** TEV13 (0.64 μl of a 2 mM stock in DMSO) was added to 40 μl of TEV buffer, and then 20 μl was taken to perform another six twofold dilutions. TEV buffer was used as a zero standard. Then 20 μl of 400 nM TEV protease and 40 μl of cell lysates were added to each well, and the samples were incubated at 30 °C for 1 h. Then, 0.8 μl of 0.1 mM Cy5–TEV13 fluorescent probe was added to each condition and incubated at 30 °C for 1 h before 30 μl of 4× SDS–PAGE sample buffer was added to each well to quench the reaction. After boiling the samples for 5 min, 15 μl of the samples from each condition was analyzed on a 12% SDS–PAGE gel. Cy5 fluorescence was measured by scanning the gel with a Typhoon 9410 Variable Mode Imager ($\lambda_{ex}$ = 633 nm, 670 BP30 filter; GE Healthcare)[47]. The fluorescence intensity of the protein bands at the expected size was analyzed using LI-COR Image Studio Lite software and plotted with OriginPro 2019 software (OriginLab Corporation). Afterwards, the gel was stained with Coomassie blue to visualize the total protein load.

**Plasma stability of TEV13.** TEV13 (10 μl of a 2 mM stock in DMSO) was added to 290 μl mouse serum (final peptide concentration was 66.7 μM in a 300-μl final volume in BALB/c mouse serum (Innovative Research)), and the mixture was incubated at 37 °C in a water bath. After 0, 1, 2, 4 and 12 h of incubation, 50 μl of sample was mixed with 100 μl of analytical-grade ethanol and kept at −20 °C for at least 1 h to precipitate the proteins and lipids in plasma. Precipitants were centrifuged in an Eppendorf 5417 centrifuge at 14,000 r.p.m. at 4 °C, and the supernatant containing the peptides was mixed with 300 μl water before being lyophilized to dryness. Finally, the samples were resuspended in 55 μl water, and 15 μl of each sample was characterized by analytical RP-HPLC on an Agilent HPLC system (1100 Series) equipped with an Agilent ZORBAX 300SB-C3 reverse-phase column. The elution linear gradient was 0–95% (vol/vol) solvent B over 14 min at a flow rate of 1 ml min$^{-1}$ (A, 99.9% (vol/vol) water and 0.1% (vol/vol) trifluoroacetic acid; B, 99.9% (vol/vol) acetonitrile and 0.1% (vol/vol) trifluoroacetic acid). The eluates were detected at a wavelength of 220 nm.

**HPLC analysis of peptide purity.** Peptide stock solutions (1 μl of 3 mM) were injected into a 1260 Infinity HPLC system (Agilent) equipped with a Poroshell 120 EC-C18 2.7-μm analytical column (Agilent, 699975-902) and run with a linear gradient of a mobile phase composed of eluent A (99.9% (vol/vol) water and 0.1% (vol/vol) trifluoroacetic acid) and eluent B (99.9% (vol/vol) acetonitrile and 0.1% (vol/vol) trifluoroacetic acid) from 5% to 95% over 6 min at a flow rate of 0.6 ml min$^{-1}$. The absorbance at a wavelength of 220 nm was used to generate plots of peptide purity.

**AMBER molecular dynamics simulation.** Homology models of TEV protease with TEV13 residues E6, P7, L8 and Y9 bound in the standard mechanism to the S6, S5, S4 and S3 subsites were built using X-ray co-crystal structure datasets using 1LVM (available at the Protein Data Bank) as a template. Non-essential water molecules and ions were deleted in the Protein Data Bank files, and the peptide ligands were truncated to retain only the P6–P3 (ENLY) residues. The remaining residues in the peptide chain were added manually in randomly extended conformation. The initial structure of the DCA–VS linker was minimized with the Gaussian 16 software package and parameterized with GAFF. Tleap was used for generating MD simulation input files, and the linkages between DCA–VS

and cysteine residues in TEV13 were manually specified. Two individual models were built when the linkage between VS and active-site cysteine was generated in *R* and *S* conformations. Force field parameters of DCA–VS and surrounding atoms were taken from GAFF, and partial charges were calculated with the HF/6-31G* RESP charge method. All structures were first minimized by holding the conformation of the TEV13 E6, P7, L8 and Y9 residues and TEV protease, followed by whole-system minimization. Then, the system was heated to 300 K before equilibration on the whole system. The production equilibration was run at 300 K with constant pressure and periodic boundary for 40 ns. Langevin dynamics was used to control the temperature using a collision frequency of 1.0 collision per ps. The final structures were analyzed, and the lowest-energy structure was presented[48]. All the calculations were performed by the AMBER biomolecular simulation package (code available at http://ambermd.org/) and were compiled in the Sherlock high-performance computing cluster provided by Stanford University and the Stanford Research Computing Center.

**Preparation of RAW cell extracts and labeling with Cy5 probes.** RAW 264.7 cells (ATCC, TIB-71) were cultured in DMEM (Gibco, 11995-073) supplemented with 10% animal serum (GeneMate, S-1200-500), 100 U $ml^{-1}$ penicillin and 100 µg $ml^{-1}$ streptomycin (Gibco, 15140148). Cells were cultured on 10-cm culture dishes (Corning, 430167) in a humidified incubator maintained at 5% $CO_2$ and 37 °C; no mycoplasma testing was performed. At around 90% confluency, cells were scraped off into either 1 ml of buffer containing 100 mM sodium acetate (pH 5.5), 2.5 mM EDTA and 2 mM DTT or 1 ml of PBS (pH 7.4) supplemented with 2 mM DTT and then lysed by ultrasound sonication. After centrifugation at 18,000*g* at 4 °C for 15 min, the supernatant was aliquotted into 60-µl fractions. Probes (0.6 µl) were added to the lysates to achieve final probe concentrations of 1 µM, 0.5 µM, 0.25 µM and 0.125 µM and incubated at 37 °C for 1 h. After adding 15 µl of SDS–PAGE sample buffer and boiling, 15 µl of each labeling mixture was analyzed on a 12% SDS–PAGE gel. Cy5 fluorescence was measured by scanning the gel on a Typhoon 9410 variable mode imager ($\lambda_{ex}$ = 633 nm, 670 BP30 filter; GE Healthcare). The fluorescence intensity of the labeled proteins was analyzed using LI-COR Image Studio Lite software and was plotted with OriginPro 2019 software (OriginLab Corporation). Afterward, the gel was stained with Coomassie blue to visualize the total protein.

**Probe concentration- and incubation time-dependent labeling.** To obtain final peptide inhibitor concentrations of 1 µM, 0.5 µM, 0.25 µM and 0.125 µM, 2 µl of 100 µM, 50 µM, 25 µM and 12.5 µM peptide inhibitors in DMSO were added to four tubes containing 200 µl of 100 nM TEV protease in buffer (50 mM Tris-Cl pH 8.0, 100 mM KCl, 1 mM EDTA, 1 mM DTT and 0.01% Triton X-100). The reaction tubes were immediately transferred to a 30 °C incubator, and after 5, 10, 20, 30, 40, 50 and 60 min, 20 µl of the reaction mixture from each condition were mixed with 10 µl SDS–PAGE sample buffer and boiled. Samples from each condition (15 µl) were resolved on a 12% SDS–PAGE gel. Cy5 fluorescence was measured using a Typhoon 9410 variable mode imager ($\lambda_{ex}$ = 633 nm, 670 BP30 filter; GE Healthcare). The fluorescence intensity of the labeled proteins was analyzed using the LI-COR Image Studio Lite software and was plotted with OriginPro 2019 software (OriginLab Corporation).

**Reporting Summary.** Further information on research design is available in the Nature Research Reporting Summary linked to this article.

## Data availability

All data presented in this manuscript are available from the corresponding author upon reasonable request. The TEV protease-expressing plasmid sequence is available at GenBank with accession number MN480436. Characterization data for cyclization linker and probes are available in the Supplementary Information. Source data are provided with this paper.

## References


39. Kapust, R. B. et al. Tobacco etch virus protease: mechanism of autolysis and rational design of stable mutants with wild-type catalytic proficiency. *Protein Eng.* **14**, 993–1000 (2001).
40. Shen, A. et al. Simplified, enhanced protein purification using an inducible, autoprocessing enzyme tag. *PLoS ONE* **4**, e8119 (2009).
41. Fellner, M. et al. Structural basis for the inhibitor and substrate specificity of the unique Fph serine hydrolases of *Staphylococcus aureus*. *ACS Infect. Dis.* **6**, 2771–2782 (2020).
42. Bellotto, S., Chen, S., Rentero Rebollo, I., Wegner, H. A. & Heinis, C. Phage selection of photoswitchable peptide ligands. *J. Am. Chem. Soc.* **136**, 5880–5883 (2014).
43. Chen, S. et al. Improving binding affinity and stability of peptide ligands by substituting glycines with D-amino acids. *Chembiochem* **14**, 1316–1322 (2013).
44. Mikolajczyk, J. et al. Small ubiquitin-related modifier (SUMO)-specific proteases: profiling the specificities and activities of human SENPs. *J. Biol. Chem.* **282**, 26217–26224 (2007).
45. Li, H. et al. Structure- and function-based design of *Plasmodium*-selective proteasome inhibitors. *Nature* **530**, 233–236 (2016).
46. Chen, S. et al. Bicyclic peptide ligands pulled out of cysteine-rich peptide libraries. *J. Am. Chem. Soc.* **135**, 6562–6569 (2013).
47. Lentz, C. S. et al. Design of selective substrates and activity-based probes for hydrolase important for pathogenesis 1 (HIP1) from *Mycobacterium tuberculosis*. *ACS Infect. Dis.* **2**, 807–815 (2016).
48. Chen, S. et al. Dithiol amino acids can structurally shape and enhance the ligand-binding properties of polypeptides. *Nat. Chem.* **6**, 1009–1016 (2014).


## Acknowledgements

We thank the Vincent Coates Foundation Mass Spectrometry Laboratory at Stanford University for providing technical assistance with mass spectrometry. We also thank D. Waugh (National Cancer Institute) for providing the TEV expression construct, pDZ2087, and C. Heinis (EPFL) for providing the phage library. This work was supported by Swiss National Science Foundation Postdoc Mobility fellowship P2ELP3_155323 P300PB_164725 (to S.C.) and by funding from National Institutes of Health grants R01 EB026285 and R01 EB026285 02S1 (to M.B.).

## Author contributions

M.B. and S.C. conceived the project and designed the experiments. S.C., S. Lovell, S. Lee and M.F. performed the experiments and analyzed the data. M.B. and S.C. wrote the manuscript with input from all authors. M.B. and P.D.M. obtained funding for the work.

## Competing interests

The authors declare no competing interests.

## Additional information

**Extended data** is available for this paper at https://doi.org/10.1038/s41587-020-0733-7.

**Supplementary information** is available for this paper at https://doi.org/10.1038/s41587-020-0733-7.

**Correspondence and requests for materials** should be addressed to M.B.

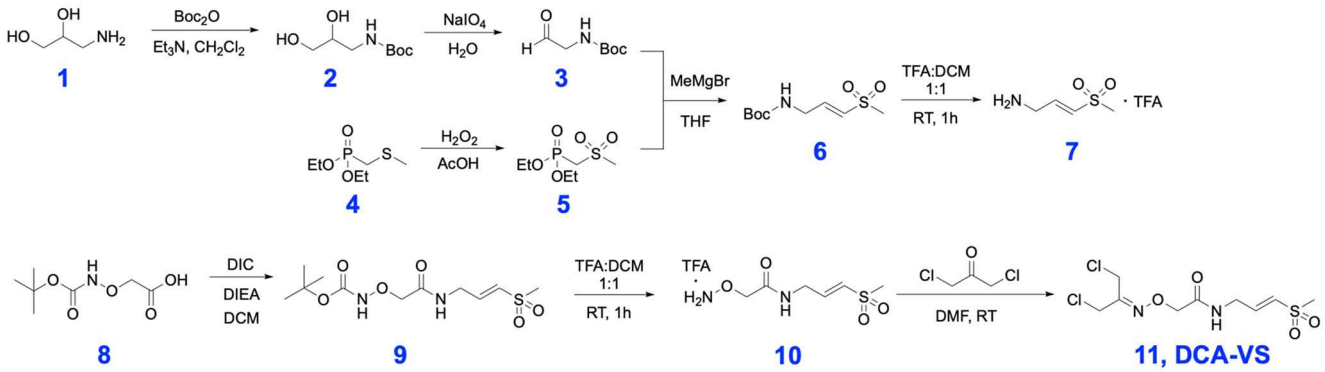


**Extended Data Fig. 1 | Strategy for the synthesis of DCA-VS, derivatizing a vinyl sulfone cysteine reactive warhead with 1,3-Dichloroacetone.** The cysteine protease reactive vinyl sulfone warhead was efficiently conjugated to the 1,2-dichloroacetone linker through oxime-ketone reaction.

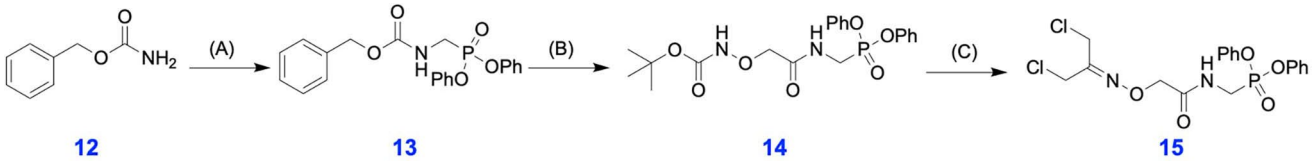


**Extended Data Fig. 2 | Strategy for the synthesis of DCA-DPP, derivatizing a diphenylphosphonate serine reactive warhead with 1,3-Dichloroacetone. a**, Acetic Anhydride, paraformaldehyde, triphenyl phosphite, acetic acid, 5 h, 120 °C, 46 % **b**, i. HBr in acetic acid ii. (Boc-aminooxy)acetic acid, DCC, DIPEA, DMF, RT, O/N, 67 % **c**, i. TFA in DCM, RT, 1 h ii. Dichloroacetone, DMF, RT, O/N, 72 %.

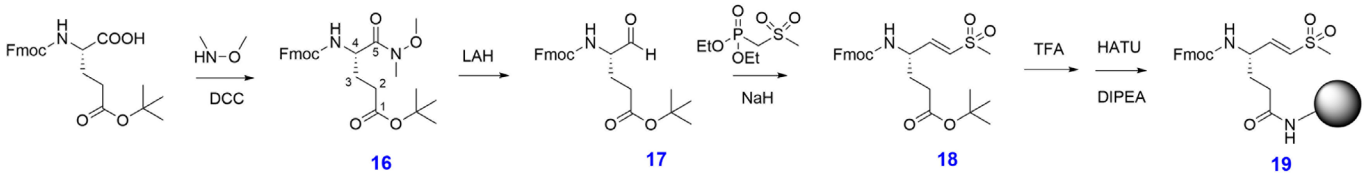


**Extended Data Fig. 3 | Strategy for synthesis of the Fmoc-Gln-vinyl sulfone warhead.** The carboxyl side chain of P1 glutamine was deprotected and reacted with chlorotrityl resin. The derived resin can be used for directly synthesizing linear ABPs bearing a glutamine-VS motif at the C-terminus.

nature research

Corresponding author(s): *Double-blind peer review submissions: write DBPR and your manuscript number here instead of author names.*

Last updated by author(s): Jun 15, 2020

# Reporting Summary

Nature Research wishes to improve the reproducibility of the work that we publish. This form provides structure for consistency and transparency in reporting. For further information on Nature Research policies, see our Editorial Policies and the Editorial Policy Checklist.

## Statistics

For all statistical analyses, confirm that the following items are present in the figure legend, table legend, main text, or Methods section.

| n/a | Confirmed | |
|---|---|---|
| ☐ | ☒ | The exact sample size (*n*) for each experimental group/condition, given as a discrete number and unit of measurement |
| ☐ | ☒ | A statement on whether measurements were taken from distinct samples or whether the same sample was measured repeatedly |
| ☒ | ☐ | The statistical test(s) used AND whether they are one- or two-sided<br>*Only common tests should be described solely by name; describe more complex techniques in the Methods section.* |
| ☒ | ☐ | A description of all covariates tested |
| ☒ | ☐ | A description of any assumptions or corrections, such as tests of normality and adjustment for multiple comparisons |
| ☐ | ☒ | A full description of the statistical parameters including central tendency (e.g. means) or other basic estimates (e.g. regression coefficient) AND variation (e.g. standard deviation) or associated estimates of uncertainty (e.g. confidence intervals) |
| ☒ | ☐ | For null hypothesis testing, the test statistic (e.g. *F*, *t*, *r*) with confidence intervals, effect sizes, degrees of freedom and *P* value noted<br>*Give P values as exact values whenever suitable.* |
| ☒ | ☐ | For Bayesian analysis, information on the choice of priors and Markov chain Monte Carlo settings |
| ☒ | ☐ | For hierarchical and complex designs, identification of the appropriate level for tests and full reporting of outcomes |
| ☒ | ☐ | Estimates of effect sizes (e.g. Cohen's *d*, Pearson's *r*), indicating how they were calculated |

*Our web collection on statistics for biologists contains articles on many of the points above.*

## Software and code

Policy information about availability of computer code

| | |
|---|---|
| Data collection | Bruker TopSpin 2.1, Typhoon scanner control V5.0, Agilent OpenLab C.01.09, BioTek Gen5 V3.05.11, Sythesis software for syro V2.01.133 |
| Data analysis | Bruker TopSpin 3.5, MestReNova 14.0.1, Geneious Prime Version 11.0.3+7, OriginPro 2019 V9.6.0.172, Agilent OpenLab C.01.09, AmberTools19, VMD 1.9.4a35, Pymol V2.3.2 |

For manuscripts utilizing custom algorithms or software that are central to the research but not yet described in published literature, software must be made available to editors and reviewers. We strongly encourage code deposition in a community repository (e.g. GitHub). See the Nature Research guidelines for submitting code & software for further information.

## Data

Policy information about availability of data

All manuscripts must include a data availability statement. This statement should provide the following information, where applicable:

- Accession codes, unique identifiers, or web links for publicly available datasets
- A list of figures that have associated raw data
- A description of any restrictions on data availability

TEV protease expressing plasmid sequence is availability at GenBank with accession number MN480436. Synthetic methods and characterizations of cyclization linker and vinyl sulfone probes are available in the Supplementary Information.

# Field-specific reporting

Please select the one below that is the best fit for your research. If you are not sure, read the appropriate sections before making your selection.

☒ Life sciences ☐ Behavioural & social sciences ☐ Ecological, evolutionary & environmental sciences

For a reference copy of the document with all sections, see nature.com/documents/nr-reporting-summary-flat.pdf

# Life sciences study design

All studies must disclose on these points even when the disclosure is negative.

| | |
|---|---|
| Sample size | In inhibitory assays, three repeat tests were performed. Three series of dilutions were performed to test the phage titers under different conditions. |
| Data exclusions | In inhibitory assays, other than the first condition of total inhibition or no inhibition was excluded. |
| Replication | Proteases labeling with various florescencent probes were performed at least twice showing similar results. |
| Randomization | not applicable |
| Blinding | not applicable |

# Reporting for specific materials, systems and methods

We require information from authors about some types of materials, experimental systems and methods used in many studies. Here, indicate whether each material, system or method listed is relevant to your study. If you are not sure if a list item applies to your research, read the appropriate section before selecting a response.

## Materials & experimental systems

| n/a | Involved in the study |
|---|---|
| ☒ | ☐ Antibodies |
| ☐ | ☒ Eukaryotic cell lines |
| ☒ | ☐ Palaeontology and archaeology |
| ☒ | ☐ Animals and other organisms |
| ☒ | ☐ Human research participants |
| ☒ | ☐ Clinical data |
| ☒ | ☐ Dual use research of concern |

## Methods

| n/a | Involved in the study |
|---|---|
| ☒ | ☐ ChIP-seq |
| ☒ | ☐ Flow cytometry |
| ☒ | ☐ MRI-based neuroimaging |

# Eukaryotic cell lines

Policy information about cell lines

| | |
|---|---|
| Cell line source(s) | HEK293 and RAW cells were purchased from ATCC. |
| Authentication | Cell lines used were not authenticated. |
| Mycoplasma contamination | Cell lines were not tested for mycoplasma contamination. |
| Commonly misidentified lines (See ICLAC register) | HEK293 was once misidentified with contaminating cell line of HeLa in 1981, and no further case was listed at ICLAC register. The HEK293 and raw cells used in this study were purchased directly from ATCC and used within 10 passages. |